Shallow Water Remote Sensing

John Hedley, IOCCG Summer Class 2022

- Overview - different methods and applications
- High spatial resolution imagery and Sentinel-2
- Empirical methods for bottom mapping and bathymetry
- Model inversion methods and uncertainty propagation
- Sun-glint correction of high spatial resolution images
- ICESat-2 data for bathymetry
- Challenges and opportunities

Objectives of shallow water remote sensing

- Bottom mapping

  - corals, seagrasses, macroalgae
- Water optical properties
- Bathymetry (depth)

Applications

- Spatial ecology (science)
- Resource mapping, MPA design, impact assessments.
- Assessing ecosystem services

  - coastal protection and stabilisation

  - fisheries, local subsistence

  - blue carbon

  - tourism

Applications on coral reefs and similar environments

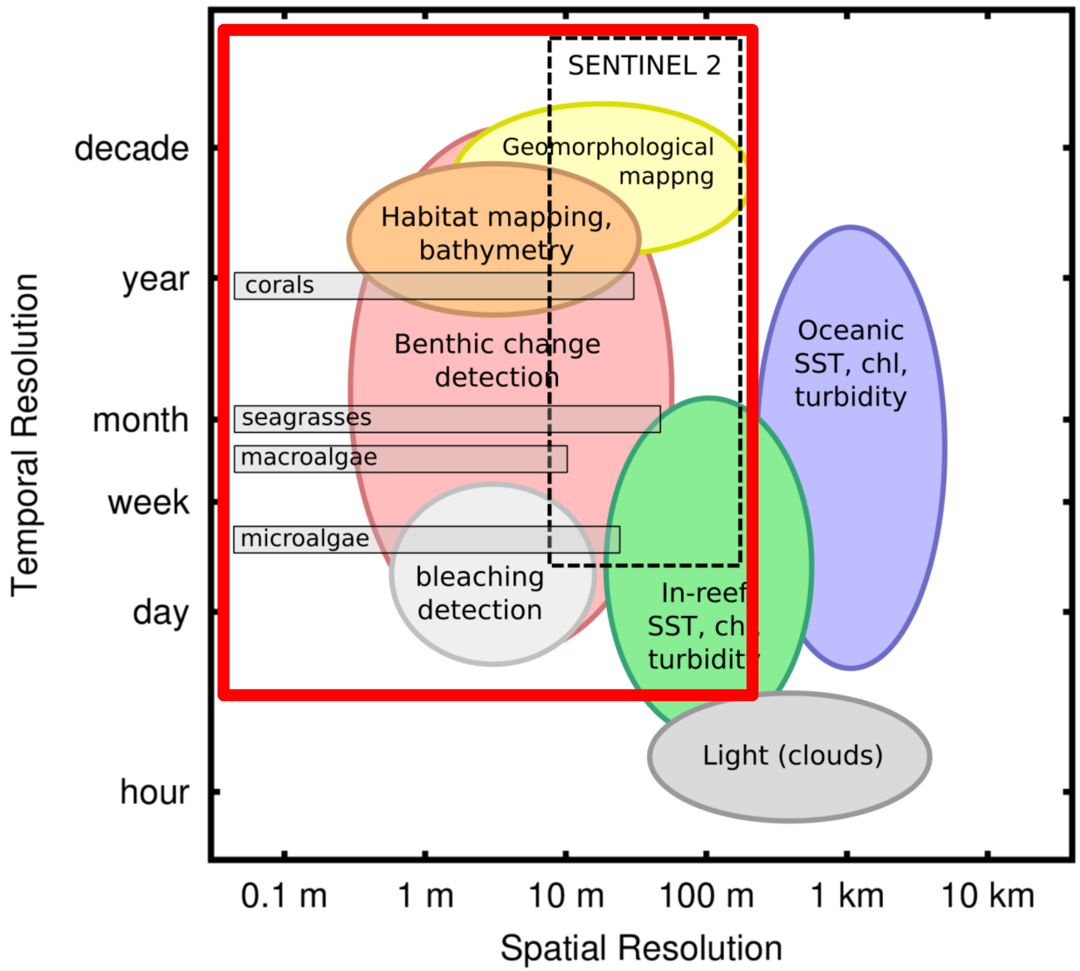

- Need higher spatial resolution than typical ocean colour satellites

Hedley et al. 2018, *RSE*, 216, 598–614

High Spatial Resolution Imagery

Pixel size < 5 m

- Many past and present (archive imagery still available)
- Pleiades, DigitalGlobe (WorldView-2, 3, 4, GeoEye, IKONOS), Planet (various)
- Typically 4 bands, R, G, B and NIR, but WorldView has 8 bands

Pixel size 10 - 30 m

- SPOT (various)
- Landsat 8 (30 m)
- Sentinel 2 (10 m in four bands)

Notes:

- Radiometric calibration on commercial satellites is often not as good as on space agency satellites.
- For these sensors bands are spectrally wide, not narrow as with ocean colour satellites
  - not always appropriate to just use centre wavelength
  - may need to integrate over wavelength

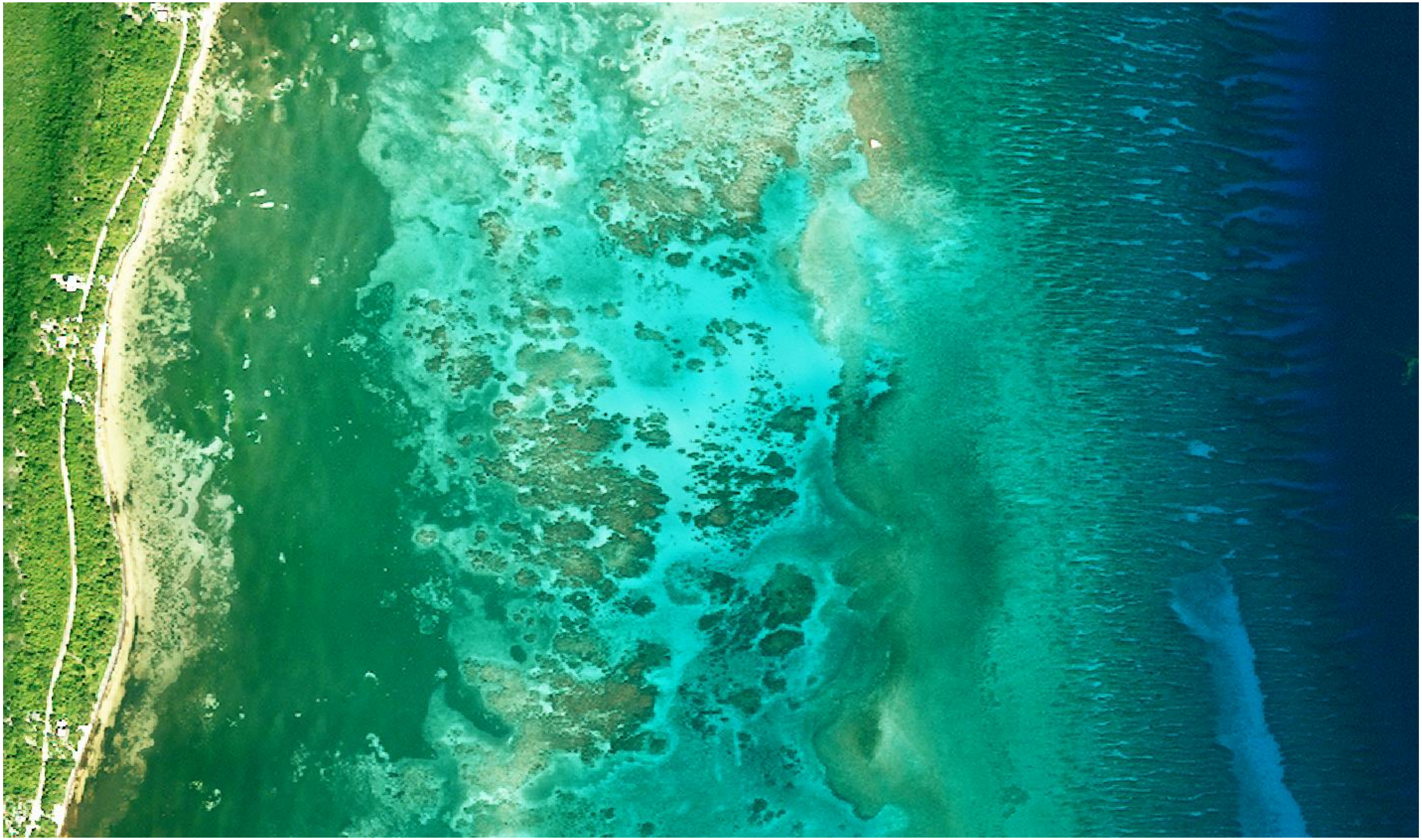

(c) DigitalGlobe

WorldView-2 image of Yucatan coast, Mexico (15 Feb 2008)
(pixels < 2 m, 8 bands, ~5 usable)

ESA / Copernicus

Sentinel-2 image of Yucatan coast, Mexico (17 April 2018)
(pixels 10 m, ~5 usable bands)

Sentinel 2 - useful bands are at different resolutions

Band	Wavelength range	Pixel size
01	433 – 453 nm	60 m
02	457 – 523 nm	10 m
03	542 – 578 nm	10 m
04	650 – 680 nm	10 m
05	697 – 713 nm	20 m
06	732 – 748 nm	20 m
07	773 – 793 nm	20 m
08	784 – 900 nm	10 m
8A	855 – 875 nm	20 m
09	935 – 955 nm	60 m

→ Interesting potential issues / artefacts

Methods for bottom mapping and/or bathymetry

Many and very diverse – overlap with terrestrial methods

Empirical, image based, requires training from in-situ data

- Classification, depth invariant indices
- Bathymetry by regression methods

Model inversion

- 'Physics based' radiative transfer models

Object orientated

- Classification combined with rules which can take data from various remote sensing methods
- e.g. depth, wave energy (wind)

Empirical image based methods (e.g. bathymetry)

- Usually assume exponential attenuation of light with depth (i.e. constant K_d)
- Requires training of points from imagery (deep water, known depths etc.)
- Similar methods for water column correction, change detection, etc.

Lyzenga 1978

$$X_i = \ln(L_i - L_{si})$$

$$Z = a_0 + a_i X_i + a_j X_j$$

a0, a1, a2 from regression

Stumpf et al. 2003

$$z = m_1 \frac{\ln(nR_w(\lambda_i))}{\ln(nR_w(\lambda_j))} + m_0$$

m0, m1, from regression

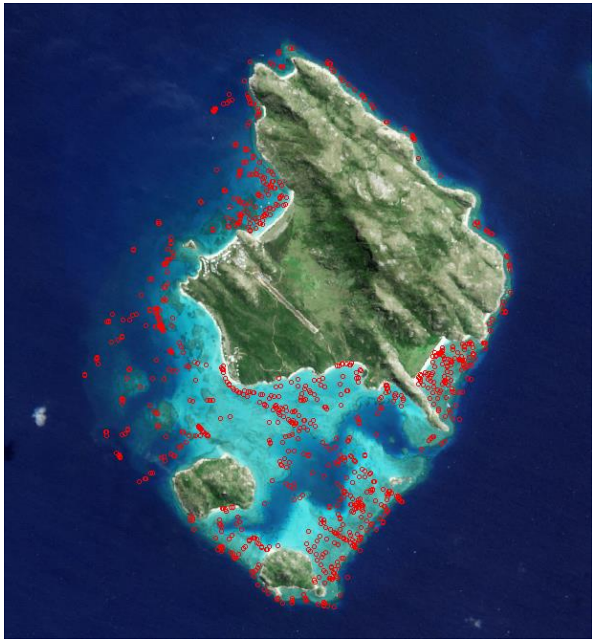

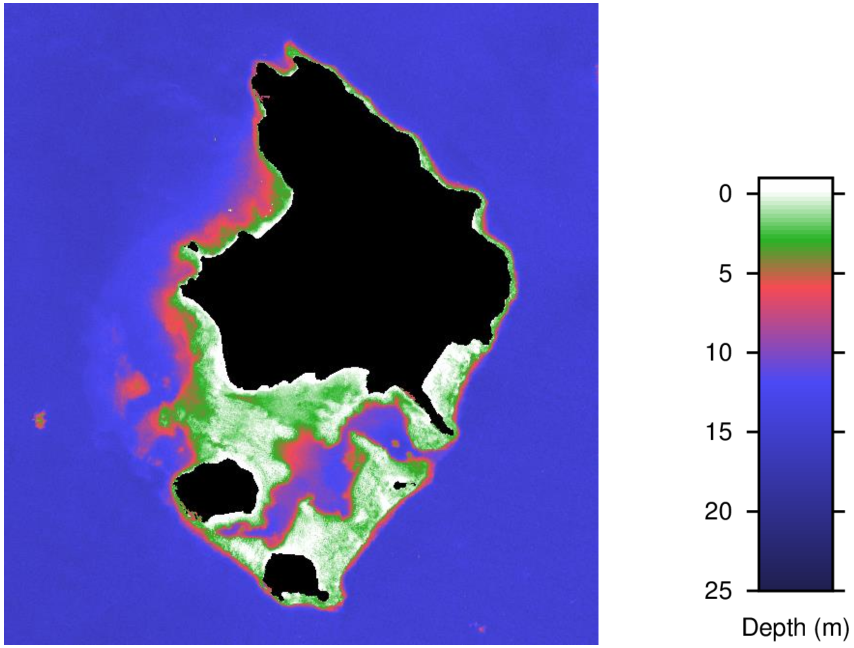

Benthic classification example, Lizard Island, GBR

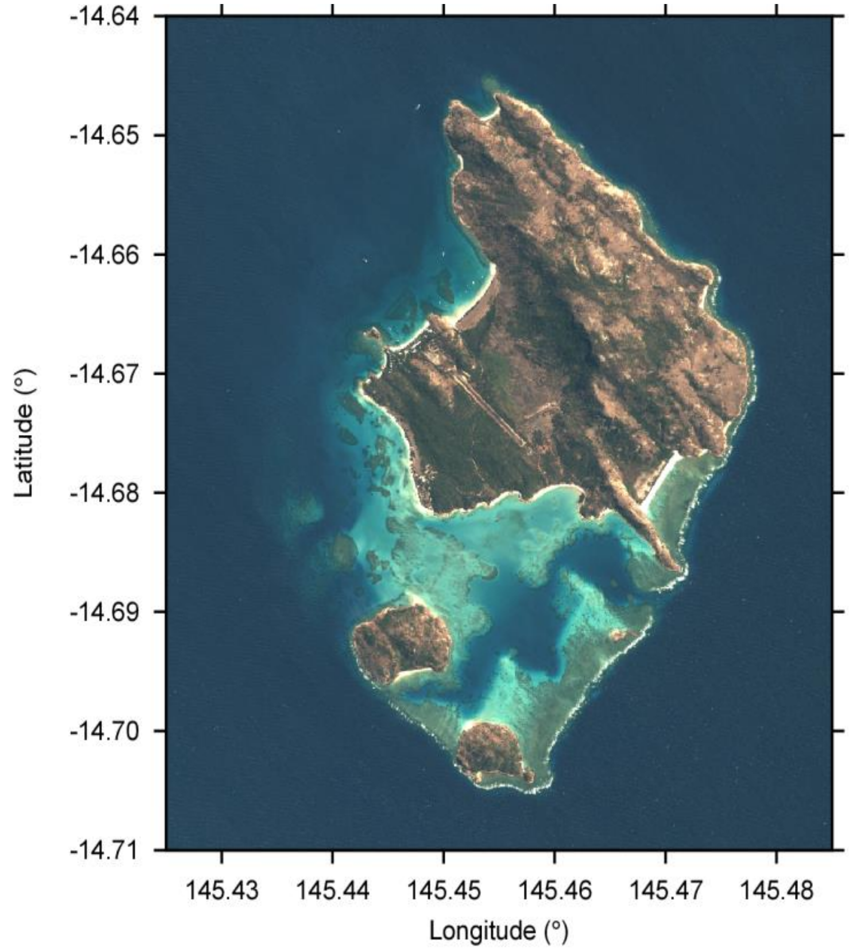

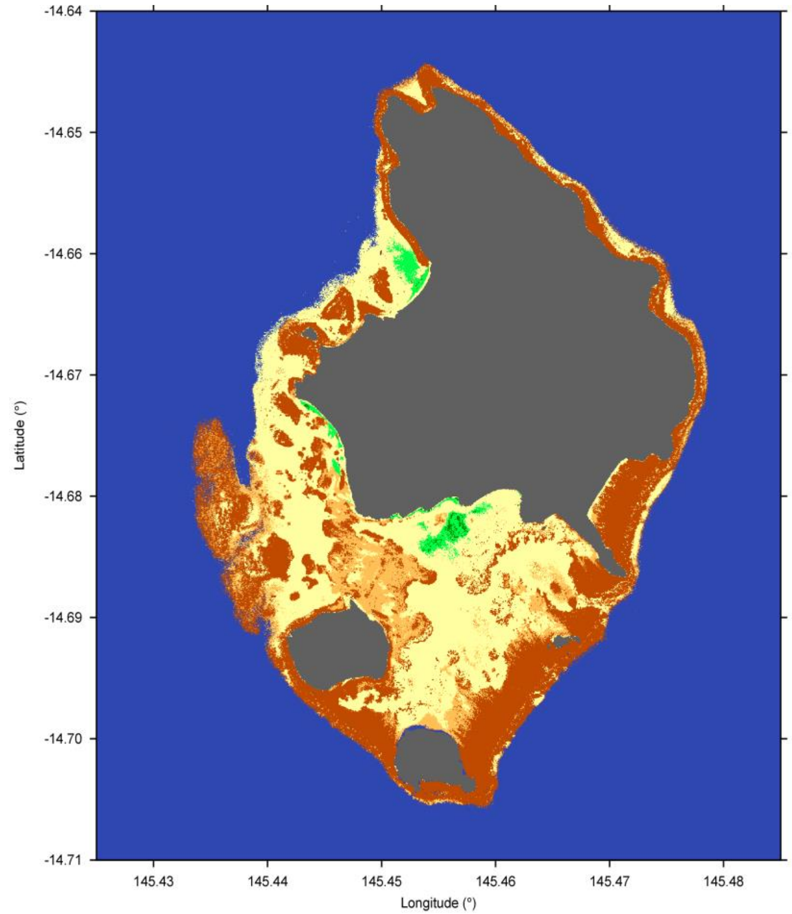

Key:

Deep Water	Medium Seagrass	Rubble / Sparse Coral
Sand	Dense Seagrass	Reef Matrix
Land		

Bottom classification - depth invariant indices

An index that should be the same for bottom types of the same reflectance at all depths

$$X_i = \ln(R_i - R_i^{\text{deep}})$$

$$X_i = \frac{k_i}{k_j} X_j + d_{ij}$$

only need <u>ratio</u> of attenuation coefficients
can extract from image using sand at different depths

Example from bands 2 and 3 of a Sentinel 2 image of Lizard Island

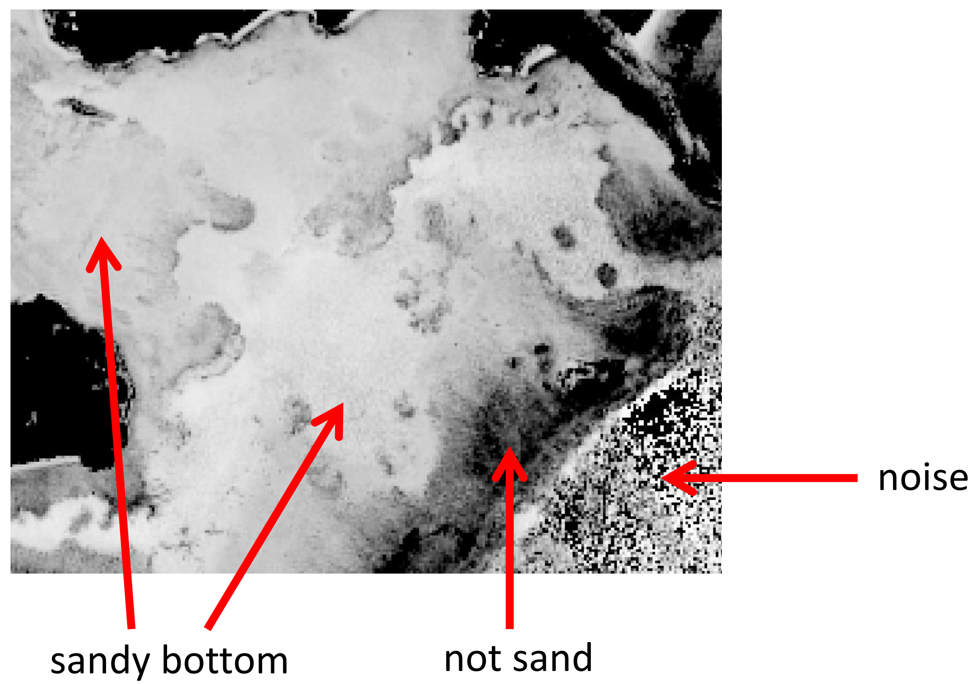

Image segmentation (object orientated methods)

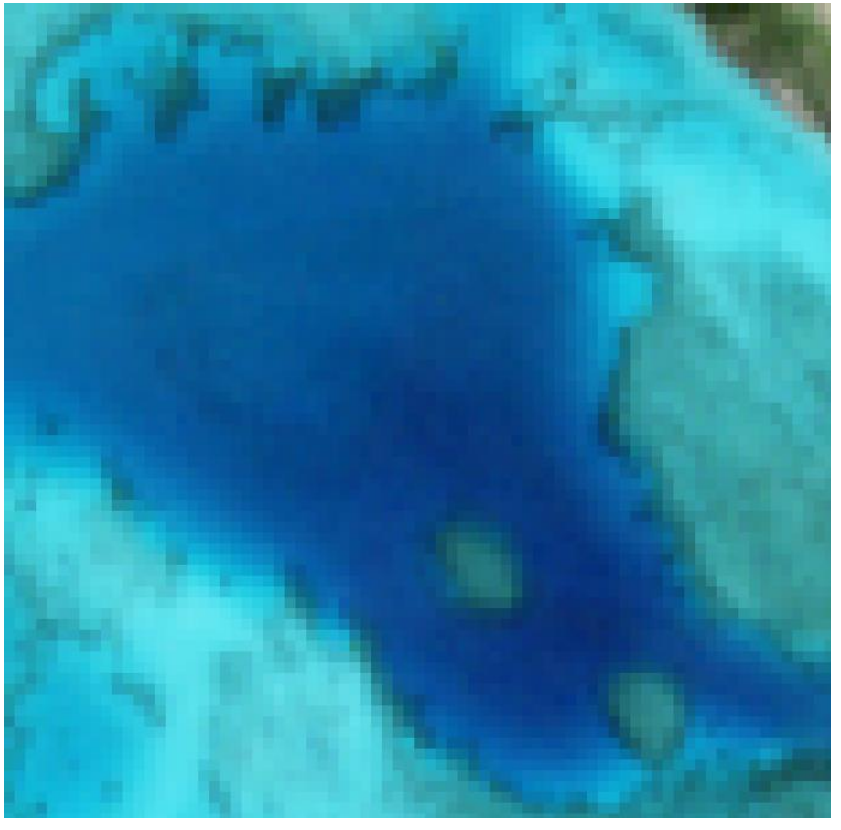

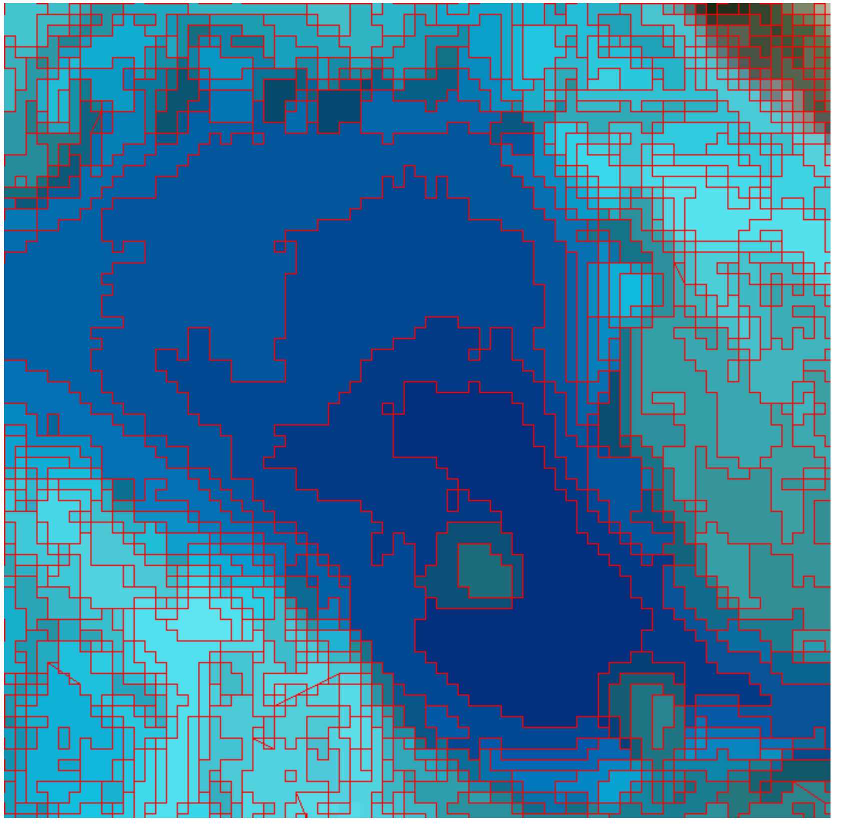

Can input object metrics into classifier, as well as image data:

- size
- shape
- orientation, etc.

Object-orientated / machine learning techniques

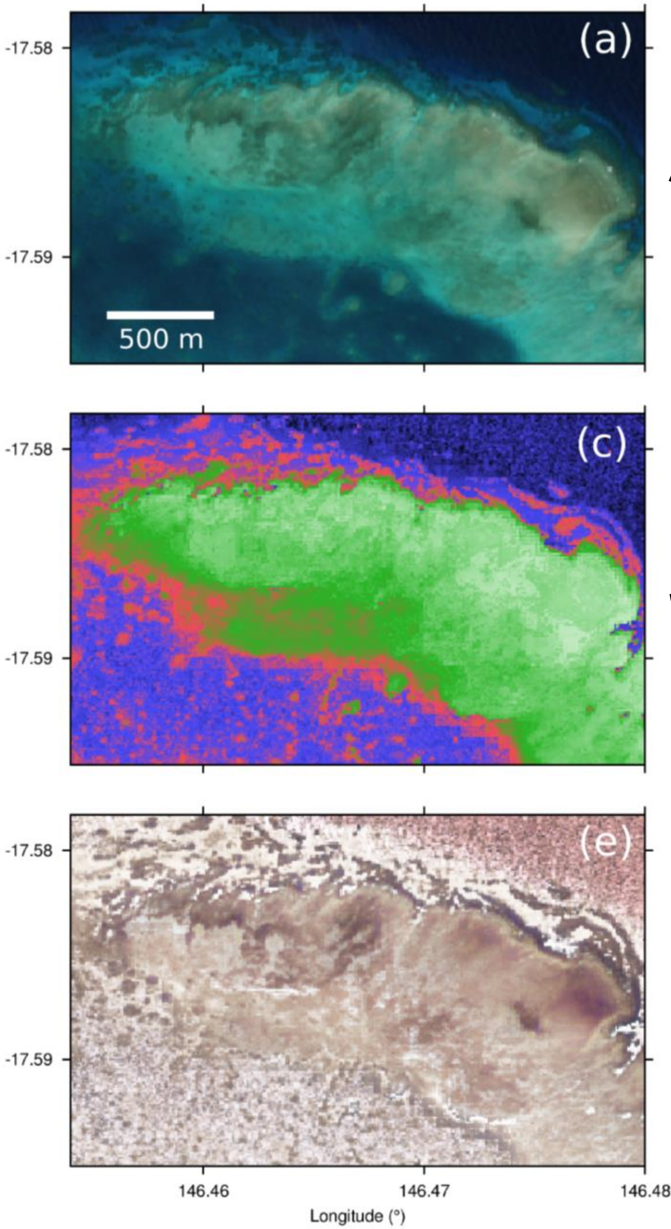

original image

bathymetry

bottom
reflectance

segmented
object metrics

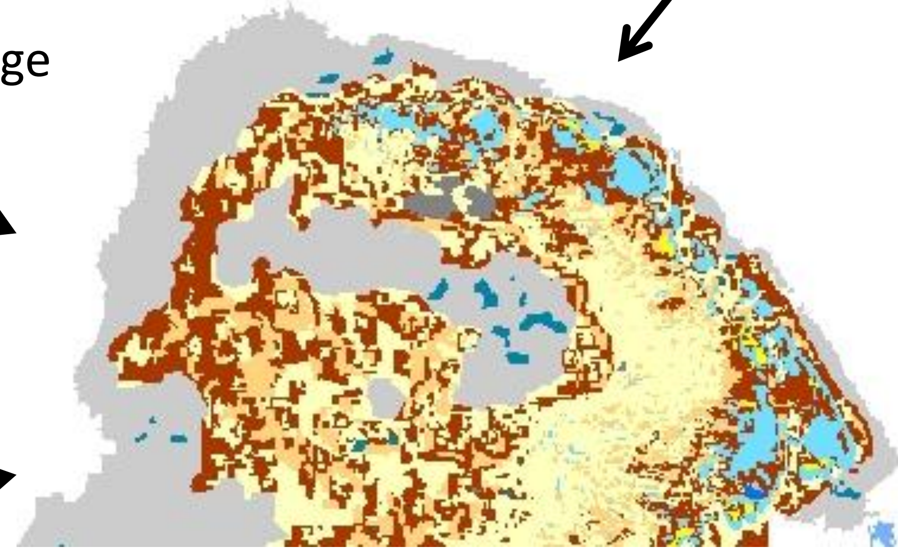

habitat map

environmental data
(e.g. wave energy, wind)

[See papers by Chris Roelfsema et al.]

Sun-glint : different types of glint dependent on spatial scale

Large images e.g. MERIS, pixels > 100 m
→ function of solar-view geometry and sea state

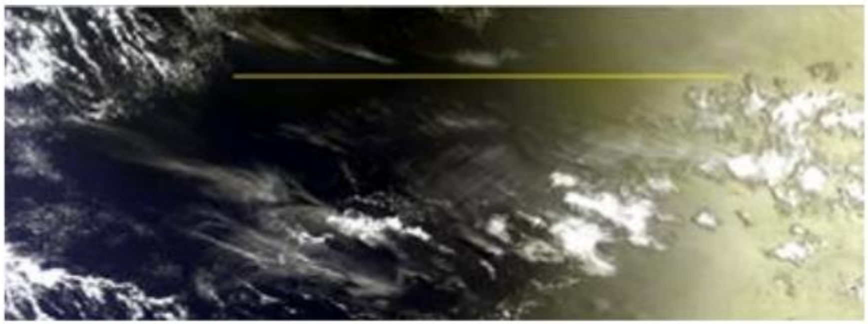

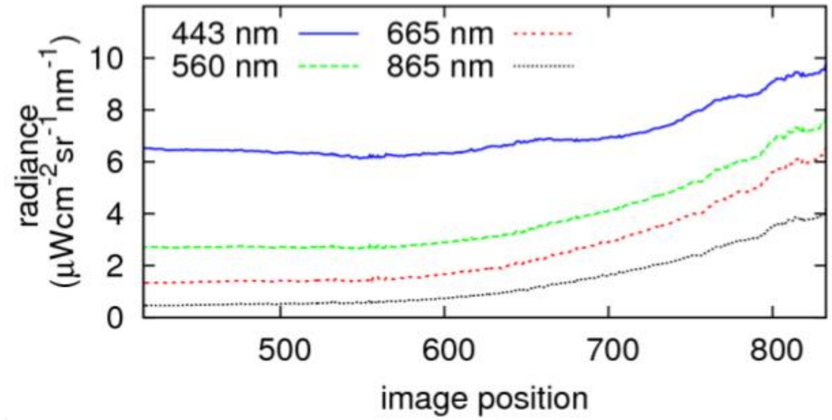

High spatial resolution, pixels < 10 m
→ individual waves

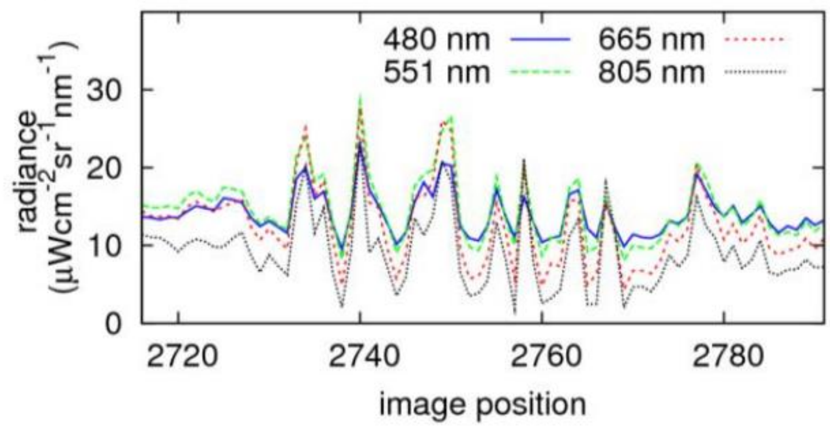

Eg. IKONOS, QuickBird, WorldView 2, Sentinel 2

Glint prediction and correction - large scale

Cox and Munk equations

- 1950s - based on photographs of surface glitter
- Many subsequent studies: all agree

Cox & Munk (1956) Slopes of the Sea Surface Deduced from Photographs of Sun Glitter. *Scripps Inst. Oceanogr. Bull*. 6(9): 401–88

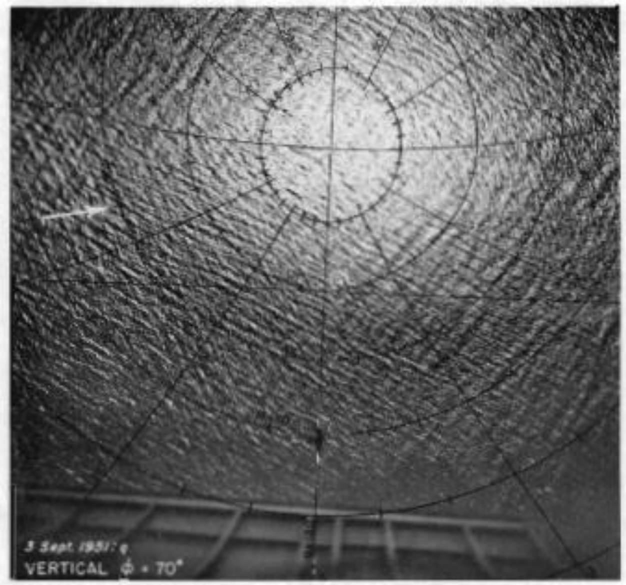

Result is statistical model of the sea surface:

Mean square slope = 0.003 + 0.00512 U_{10}

wind speed ms^{-1}

Sun-glint depends only on:

1) sun position
2) sensor position
3) wind speed (and to a small extent wind direction)

- Statistical description at large scales and open ocean → large pixels (100s m)
- No use for high resolution imagery and shallow areas

Glint correction or “deglint” of high spatial resolution images

- Can correct using a Near-Infra Red (NIR) band to assess the glint
- **Assumption 1** - Glint has a uniform spectral signature
- **Assumption 2** - NIR from below the water surface is zero

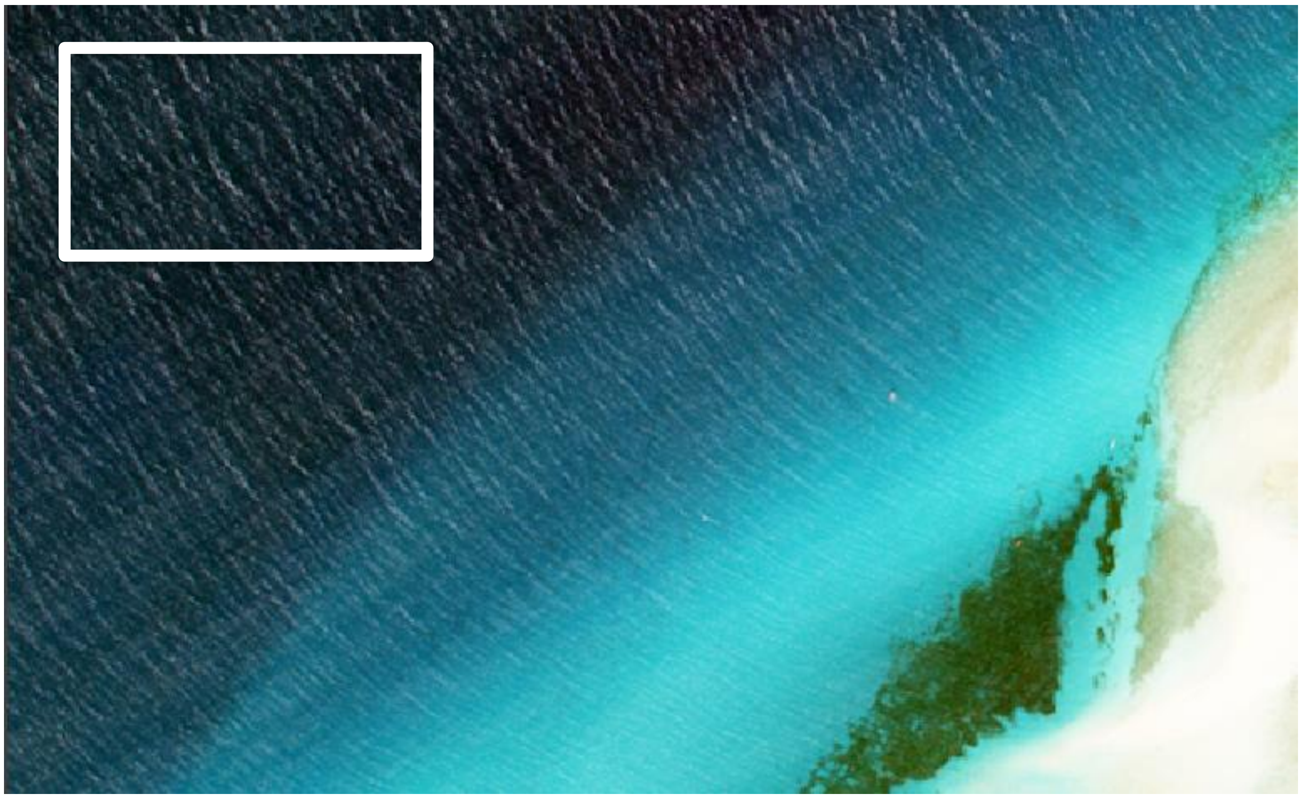

WorldView-2 Image
(c) DigitalGlobe

pixels ~2 m

- Start with a sample of pixels over deep water, where it is assumed there is no sub-surface variation in reflectance

Glint correction or “deglint” of high spatial resolution images

Sample over deep water

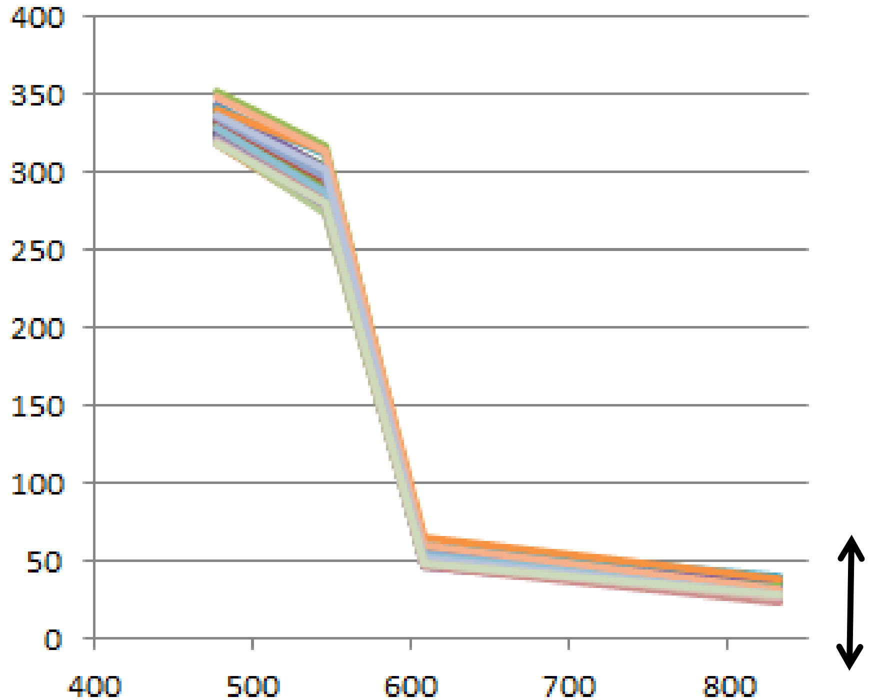

NIR reflectance (or SWIR)

Hedley et al. (2005) *International Journal of Remote Sensing* 26: 2107-2112
and other similar methods - see Kay et al. (2009) *Remote Sensing* 1: 697-730

Glint correction or "deglint" of high spatial resolution images

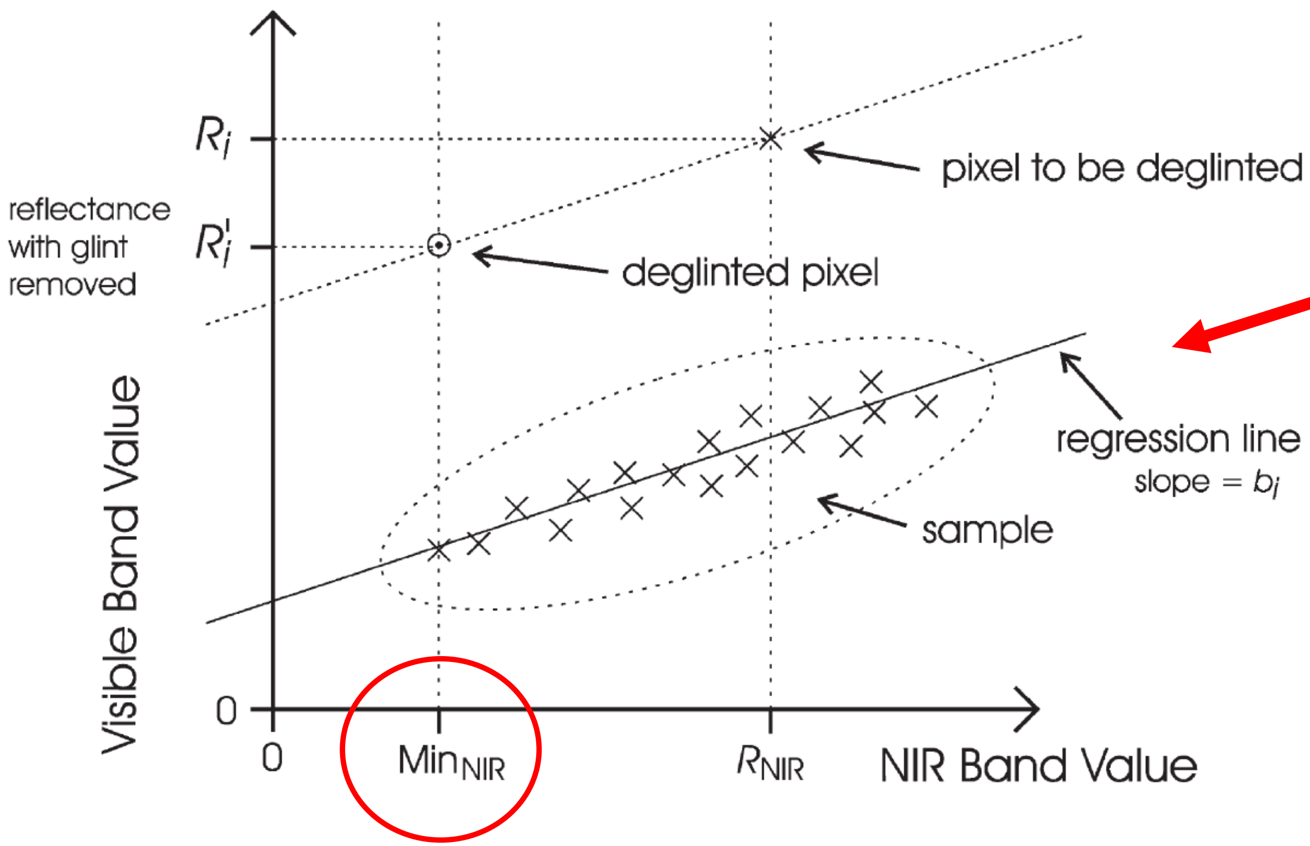

Sample over deep water

$$R_i' = R_i - b_i(R_{\text{NIR}} - \text{Min}_{\text{NIR}})$$

- Before or after atmospheric correction? – using minimum NIR reflectance means it probably doesn't matter if you assume uniform atmospheric contribution

Before deglint

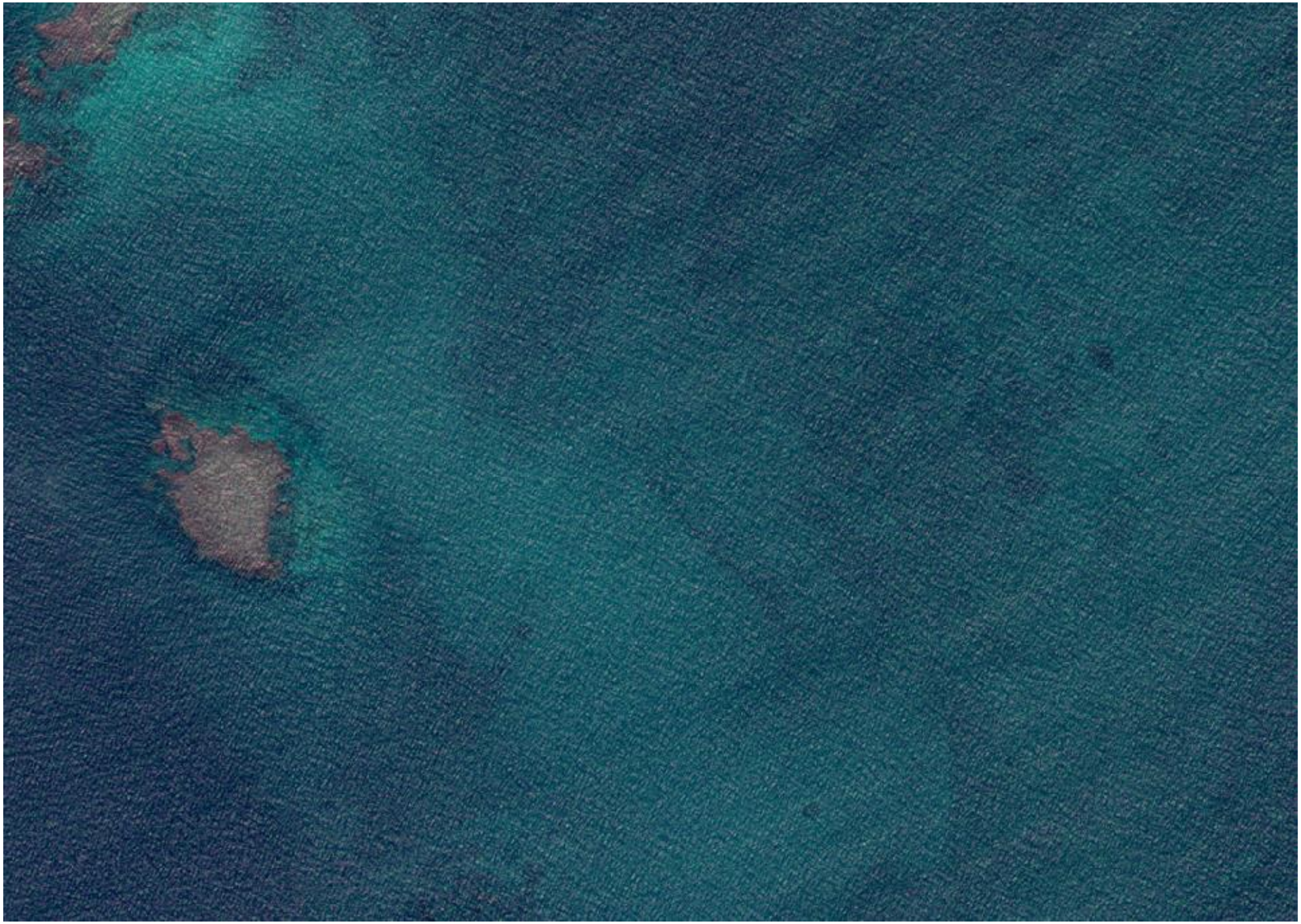

After deglint

Deglint example (Landsat 8)

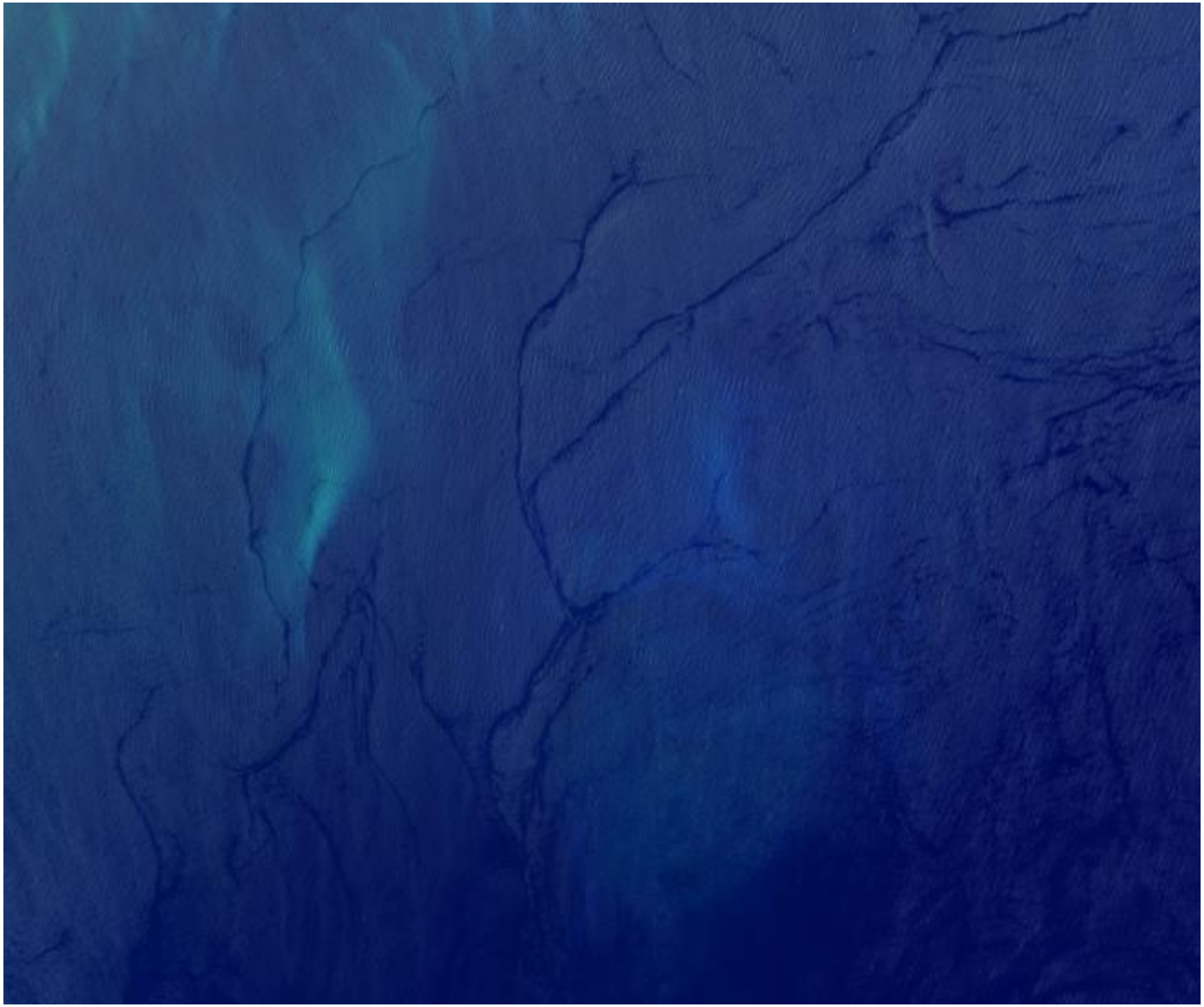

Deglint example (Landsat 8)

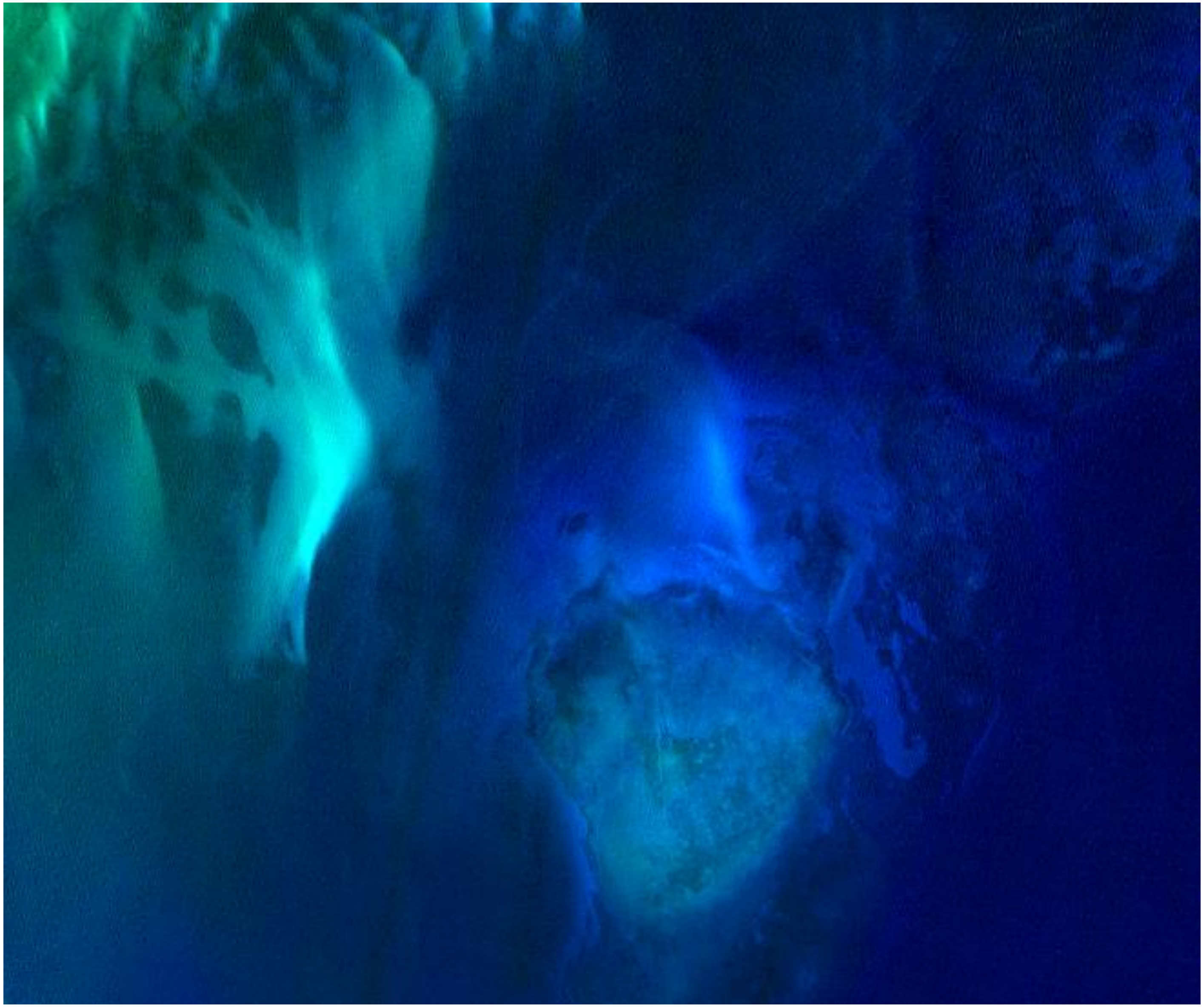

Glint corrected images are quite noisy

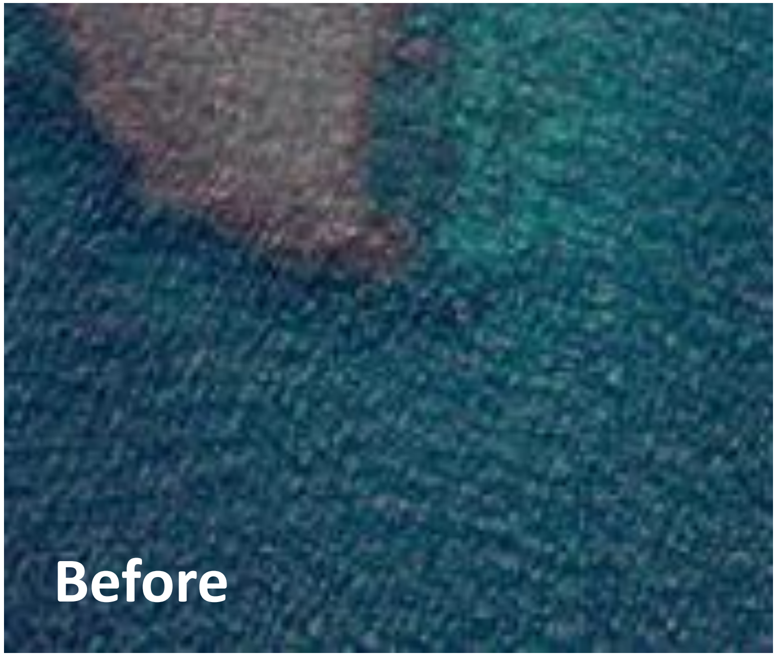

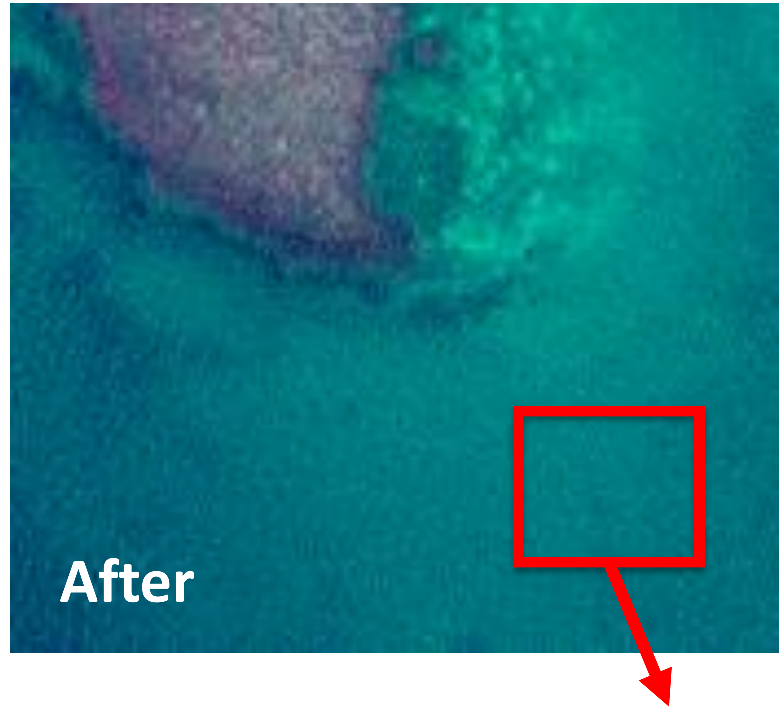

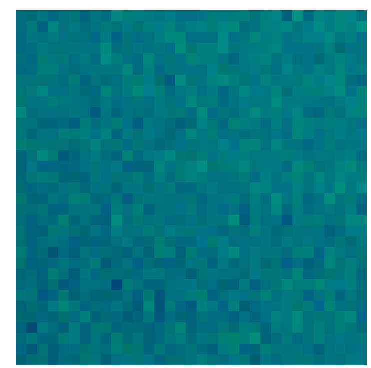

Pixel-to-pixel noise

1) Signal to noise issue - take a big signal away to leave a small signal, but noise was on the big signal.
2) Also, combining noise from two bands - visible band and NIR band.
3) Process is not perfect - band alignment, etc.

→ Spatial filtering (smoothing) may be useful

Over-correction when NIR below surface is not zero

- Assumption of zero NIR from below the water is not valid in shallow water
- Result is “dark halo” effect around land features
- Causes problems for subsequently applied algorithms

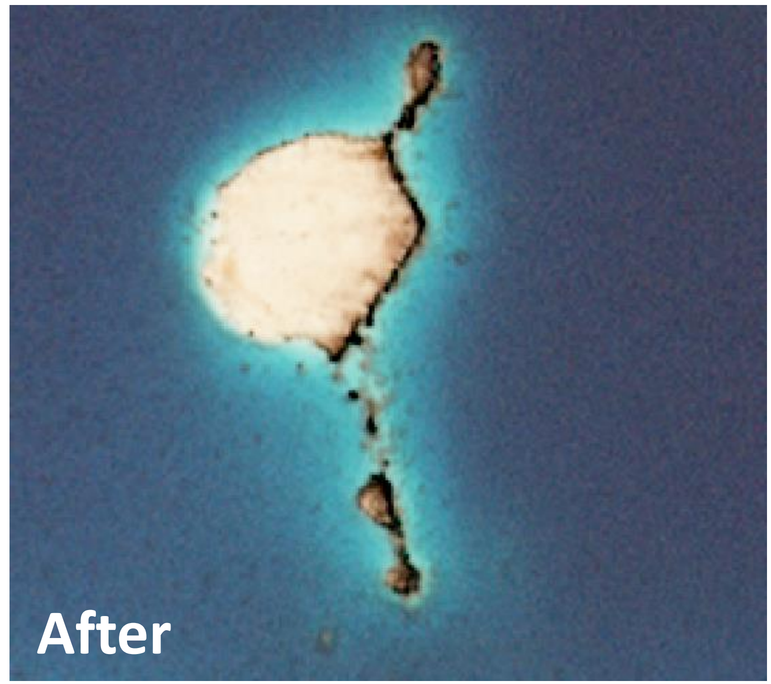

Specific challenges with Sentinel-2

Pixel size means hard to get a "no glint" reference

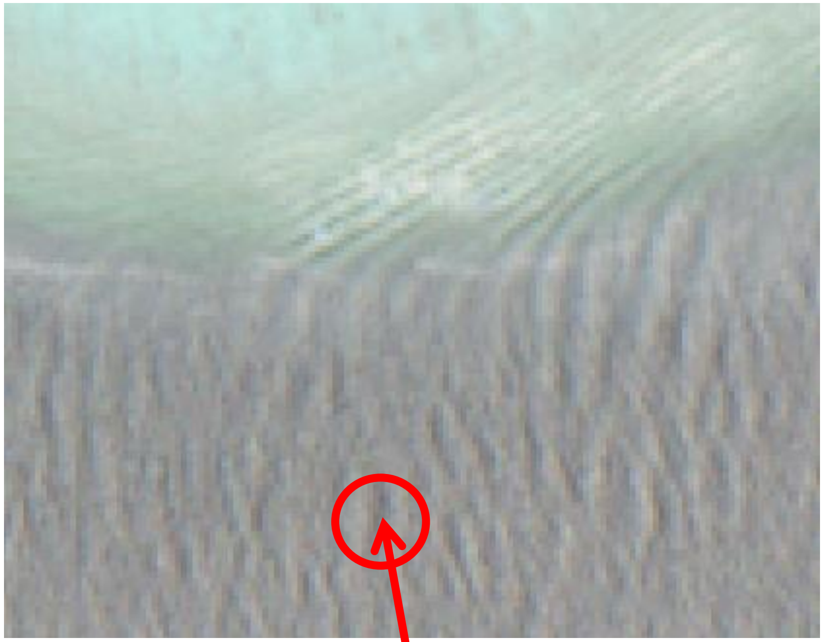

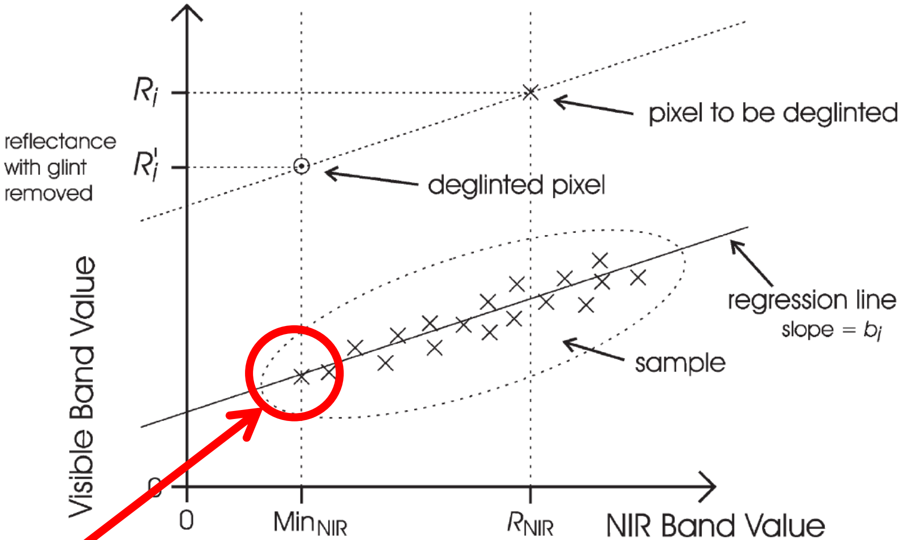

The darkest pixels probably still contain some glint

So glint correction is incomplete and there remains a glint contribution

Specific challenges with Sentinel-2

PIxel size means hard to get a “no glint” reference

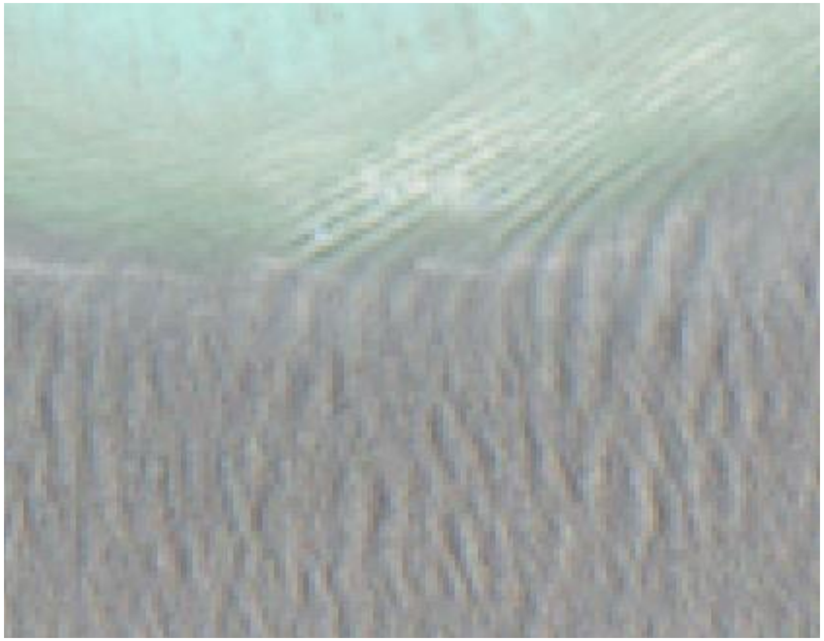

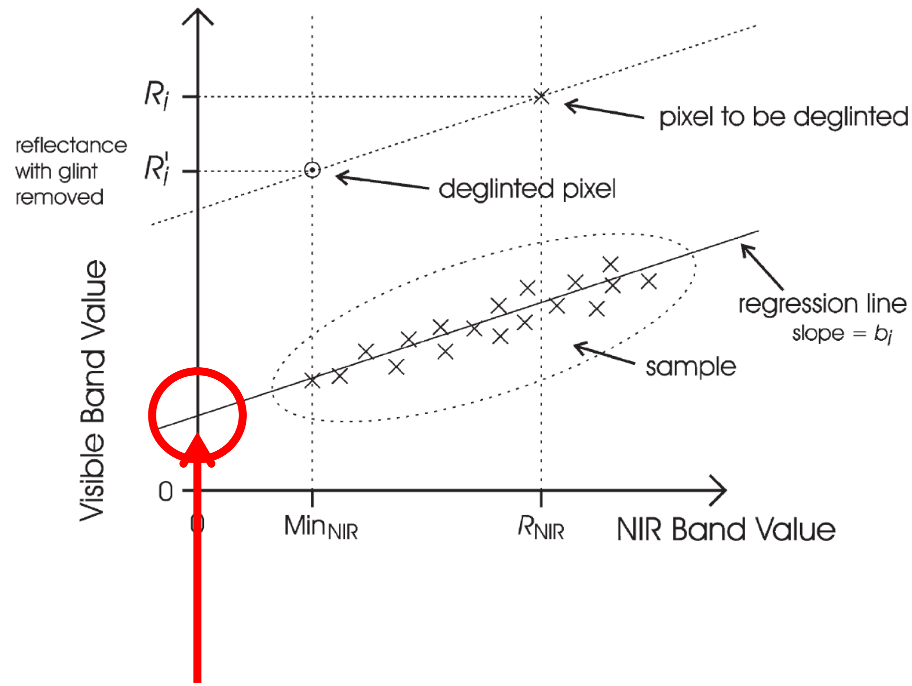

Force correction to assume zero NIR reflectance rather than empirical minimum

<u>But</u> that assumes NIR really should be zero

- i.e. atmospheric correction has removed any aerosol contribution in the NIR
- but atmospheric corrections often use NIR to estimate aerosol!

- **Very difficult to disentangle glint from aerosol contribution in Sentinel-2 imagery - without additional information**

Atmospheric reflectance, Marine 99% RH aerosol model (libRadtran)

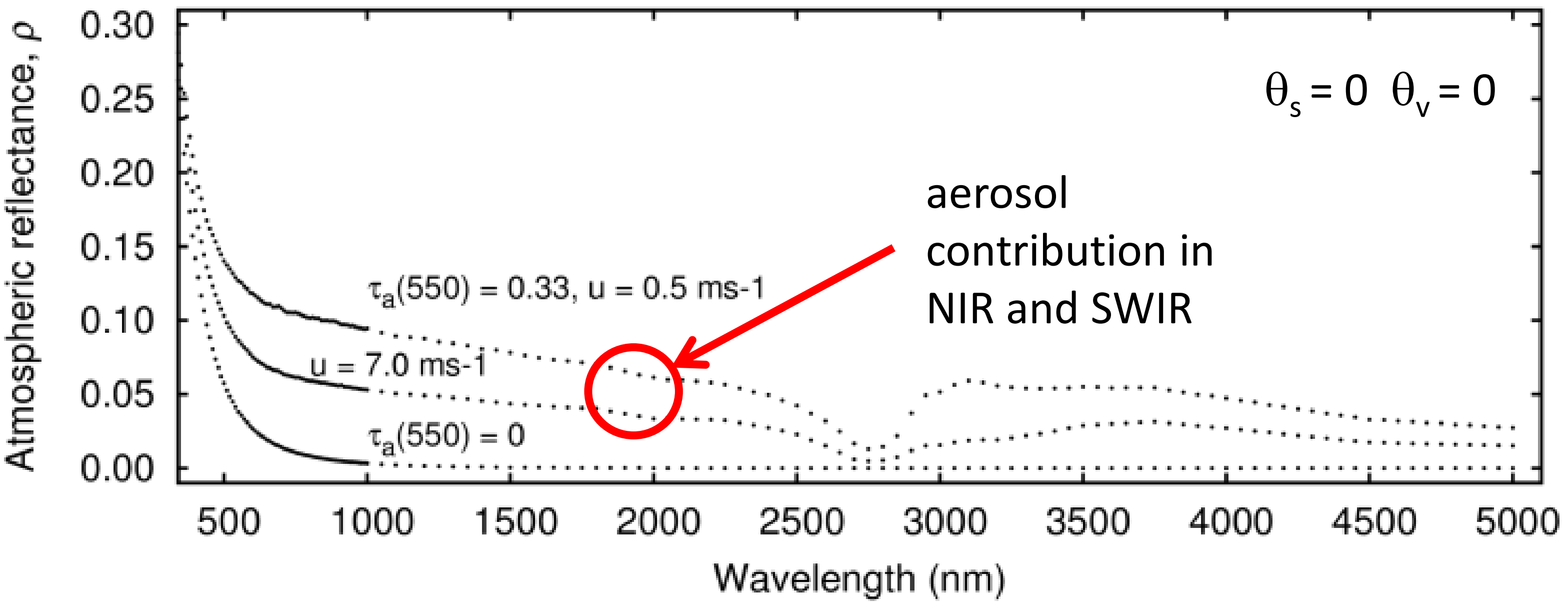

- In this plot sun and view are directly overhead (zenith and nadir)
- Indirect surface reflectance but no direct glint included
- Top two lines include aerosols, bottom line Rayleigh only

SWIR doesn't help much - there still is an aerosol and glint contribution

Use ancillary data

- Glint correction for Sentinel-2
- Uses SWIR to characterise glint
- Wavelength dependence based on refractive index of water
- Relies on a-priori separation of atmospheric reflectance from surface glint

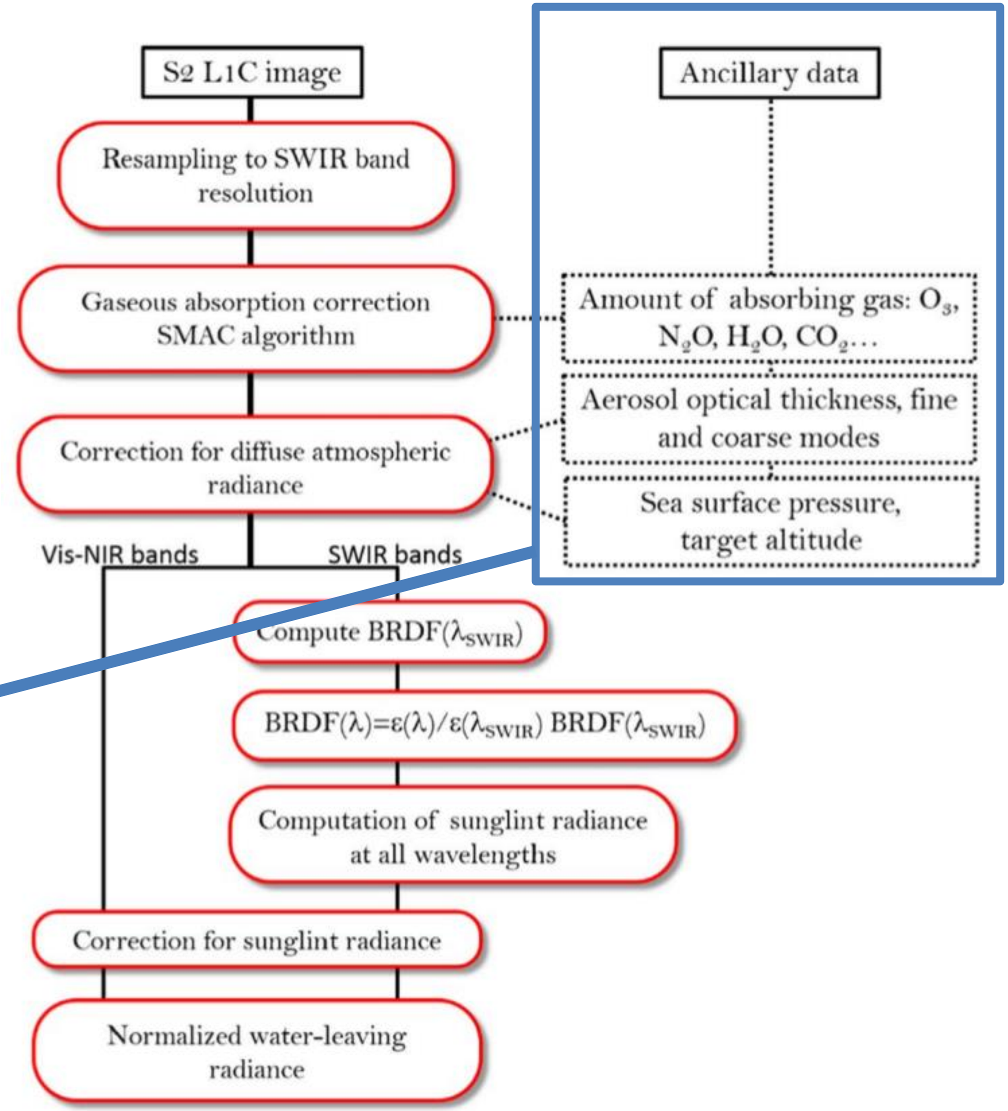

Need this data for atmospheric correction, e.g. from AERONET station.

Effectively this adds information to reduce uncertainty between aerosol and glint

Harmel T. et al. (2018) *Remote Sensing of Environment*, 204: 308-321 doi: 10.1016/j.rse.2017.10.022

Inversion methods for shallow water applications

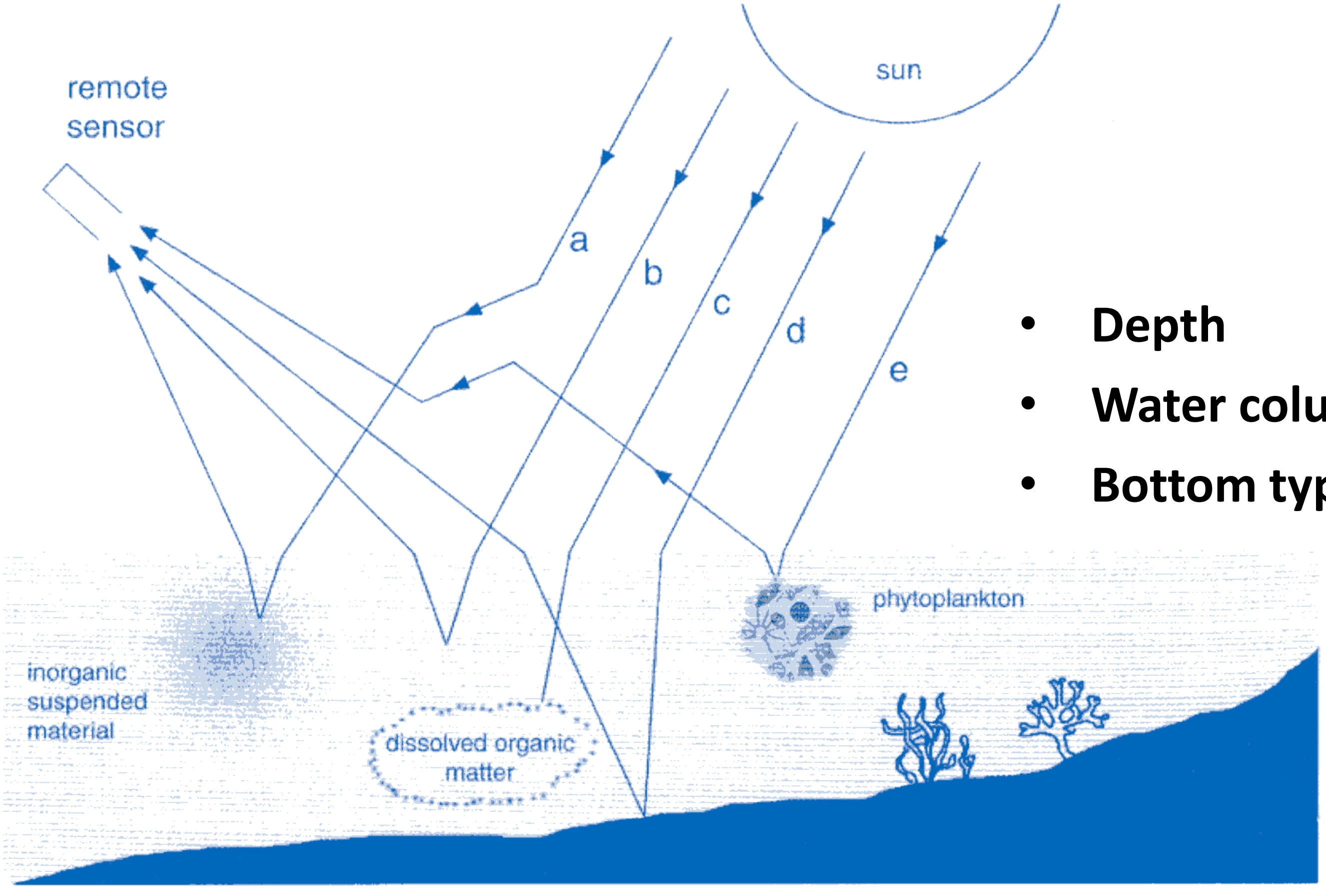

- **Depth**
- **Water column constituents**
- **Bottom type (sand, coral, etc.)**

Go from image $R_{rs}(\lambda)$ to model inputs = model inversion

Shallow water models for R_{rs}

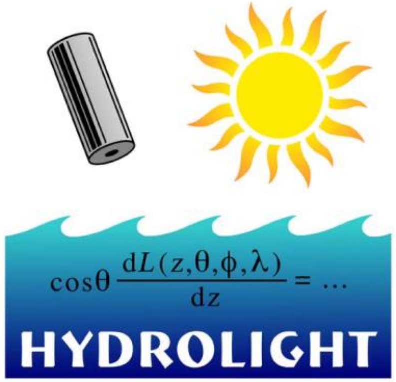

1) HydroLight-EcoLight

Build look-up tables for different depths, water column optical properties and bottom reflectances

Mobley et al. (2005) *Applied Optics* 44, 3576-3592

2) Semi-analytical models

Develop a simpler conceptual model and estimate coefficients or parameters from a physically exact model such as HydroLight

Results in a forward model that is faster to compute

Lee et al. (1998) *Applied Optics* 37, 6329-6338

Spectral Matching (LUT)

Depth,	Phytoplankton,	CDOM, … etc
1 m	0.1 mg m^{-3}	
2 m	0.1 mg m^{-3}	
3 m	0.1 mg m^{-3}	
4 m	0.1 mg m^{-3}	
1 m	0.2 mg m^{-3}	
2 m	0.2 mg m^{-3}	
3 m	0.2 mg m^{-3}	
4 m	0.2 mg m^{-3}	
1 m	0.4 mg m^{-3}	
2 m	0.4 mg m^{-3}	
3 m	0.4 mg m^{-3}	
4 m	0.4 mg m^{-3}	

MODEL

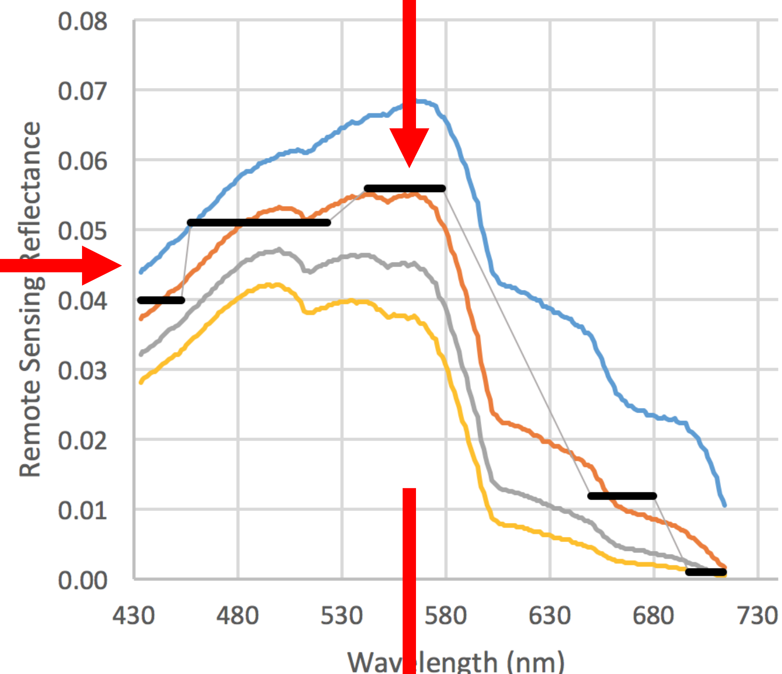

Estimate:
Depth = 2 m
Phytopankton = 0.2 mg m^{-3}
... etc

- No in-situ calibration data required.

Lee et al's semianalytical model for shallow water reflectance

$$r_{\mathrm{rs}}(\lambda) \approx f(P, G, X, H, \rho(\lambda), \lambda)$$

$$a(\lambda) = a_{\mathrm{w}}(\lambda) + [a_0(\lambda) + a_1(\lambda) \ln P]\, P + G \exp[-0.015\,(\lambda - 440)]$$

$$b_{\mathrm{b}}(\lambda) = b_{\mathrm{bw}}(\lambda) + X\,(400/\lambda)^Y$$

$$u(\lambda) = b_{\mathrm{b}}(\lambda) / [a(\lambda) + b_{\mathrm{b}}(\lambda)]\,, \qquad \kappa(\lambda) = a(\lambda) + b_{\mathrm{b}}(\lambda)$$

$$r_{\mathrm{rs}}^{\mathrm{dp}}(\lambda) \approx [0.084 + 0.170 u(\lambda)]\, u(\lambda)$$

$$D_{\mathrm{u}}^{\mathrm{C}}(\lambda) \approx 1.03\sqrt{1 + 2.4 u(\lambda)} \qquad D_{\mathrm{u}}^{\mathrm{B}}(\lambda) \approx 1.04\sqrt{1 + 5.4 u(\lambda)}$$

remote sensing reflectance

$$r_{\mathrm{rs}}(\lambda) \approx r_{\mathrm{rs}}^{\mathrm{dp}}(\lambda)\left(1 - \exp\left\{-\left[\frac{1}{\cos\theta_{\mathrm{w}}} + \frac{D_{\mathrm{u}}^{\mathrm{C}}(\lambda)}{\cos\theta}\right]\kappa(\lambda) H\right\}\right) + \frac{1}{\pi}\rho(\lambda)\exp\left\{-\left[\frac{1}{\cos\theta_{\mathrm{w}}} + \frac{D_{\mathrm{u}}^{\mathrm{B}}(\lambda)}{\cos\theta}\right]\kappa(\lambda) H\right\}$$

bottom reflectance

H = depth in metres

P = phytoplankton concentration (proxy)

G = dissolved organic matter concentration (proxy)

X = backscatter

Y = (spectral slope of backscatter) is fixed at 1

Also incorporates sun and view zenith angles

Various factors derived from HydroLight

Bottom reflectance can be treated as a mix of types

- Use pairs selected from a small spectral library
- Then mixture is just one parameter, *m,* ranging 0 to 1
- Another parameter, *E*, specifies which particular pair are used.

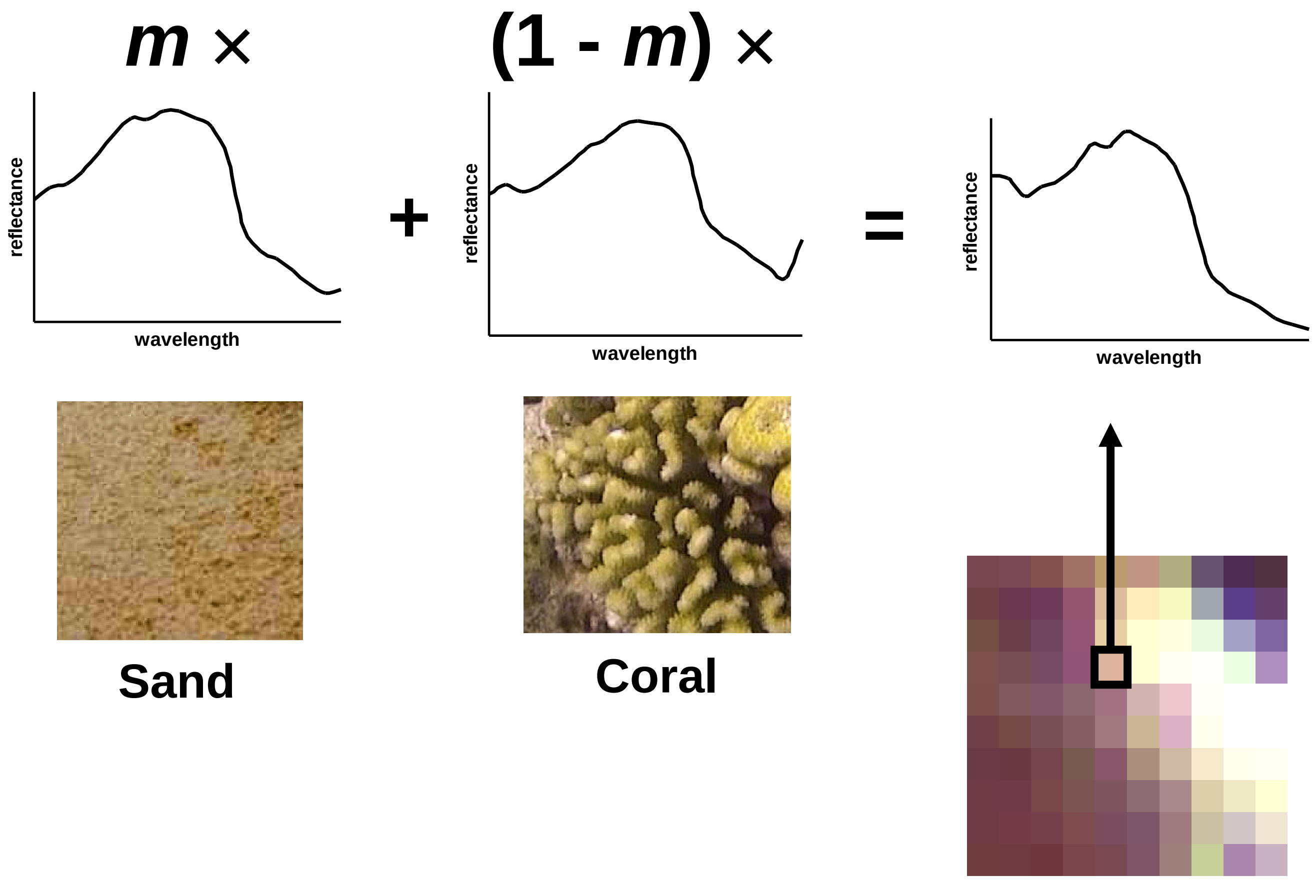

Inversion of the model

This is a **forward model** it describes what can occur in every individual pixel based on what is in the pixel

$$r_{\mathrm{rs}}(\lambda) \approx \underbrace{f(P, G, X, H, m, E)}_{\text{Six values describe every pixel}}(\lambda)$$

But we start with this
and wish to deduce this

Successive approximation technique such as the Levenberg-Marquardt algorithm, keeps adjusting inputs to find the best match for the pixel $r_{rs}(\lambda)$

Uncertainty Propagation

Fundamental uncertainty

$\rightarrow$ similar spectra from differing parameters

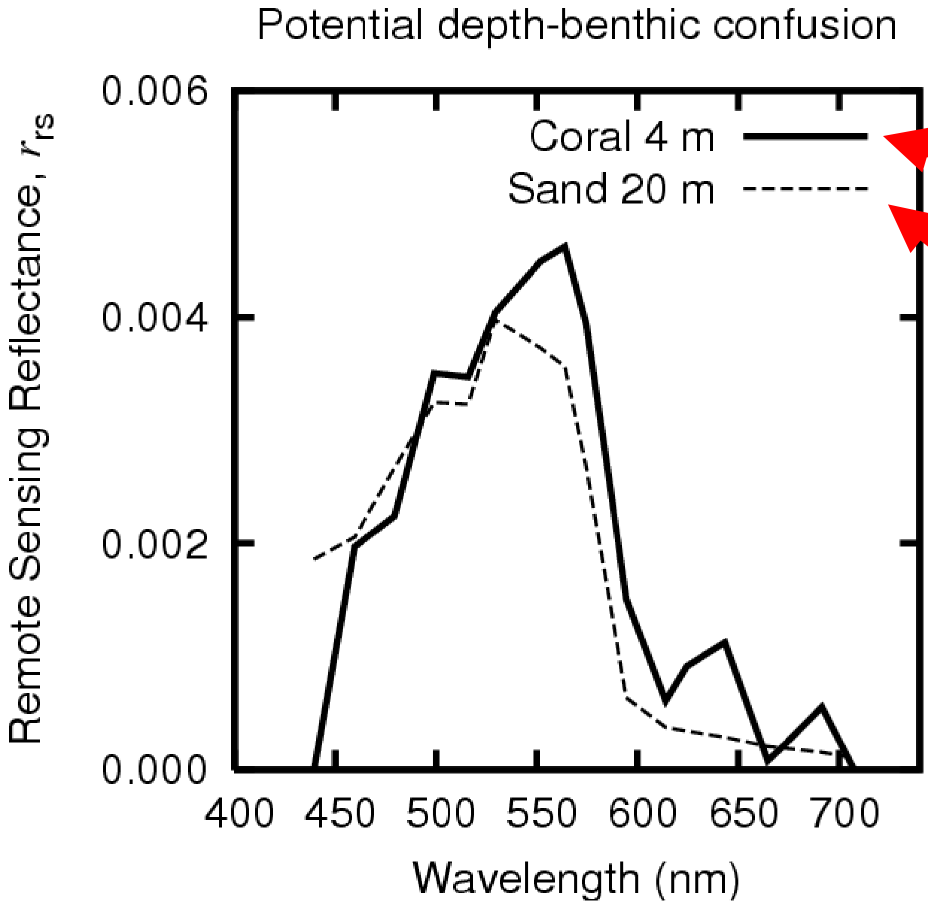

Sources of "noise" → uncertainty

Hyperspectral deep water pixels

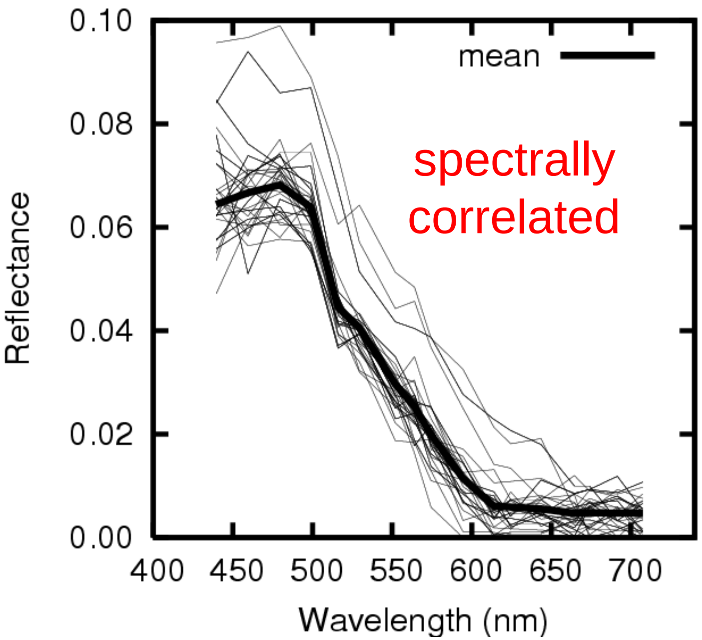

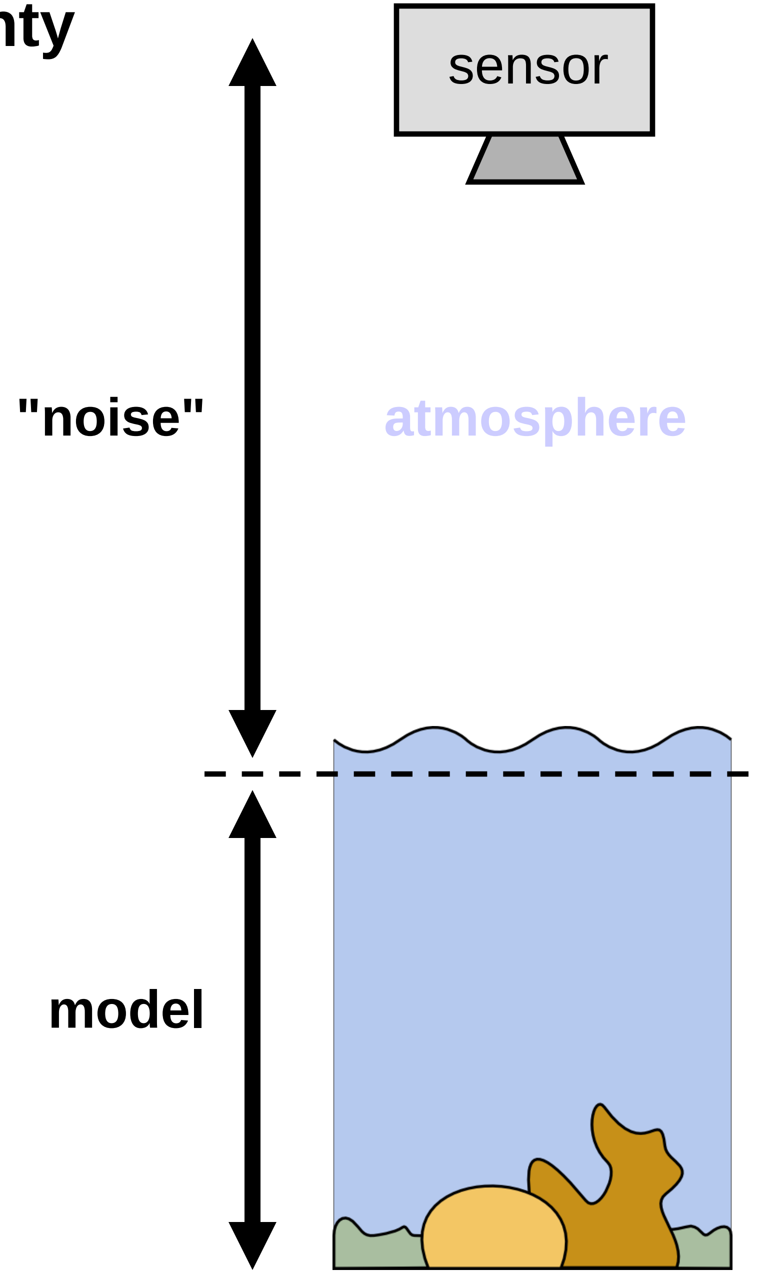

Propagation through inversion

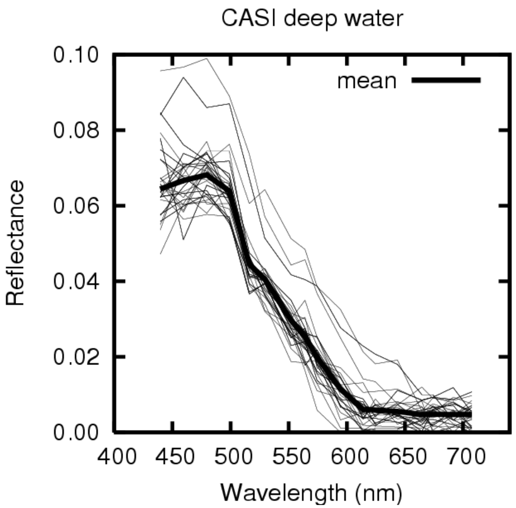

image noise

(multivariate normal)

subtract random noise term × 20 times

20 reflectance spectra

invert to retrieve parameter estimations

discard upper and lower tails to give 90% conf. intervals

use mean for actual result

- better than direct result
- spatially smoother

Bathymetry estimation with uncertainty

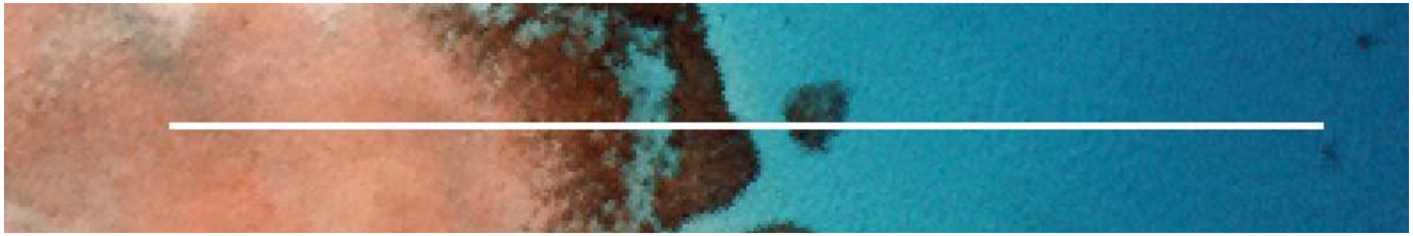

CASI

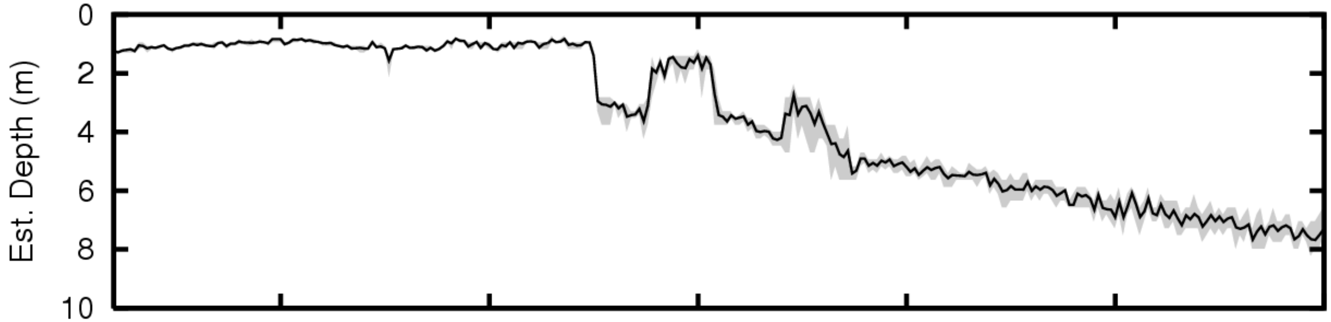

Quickbird

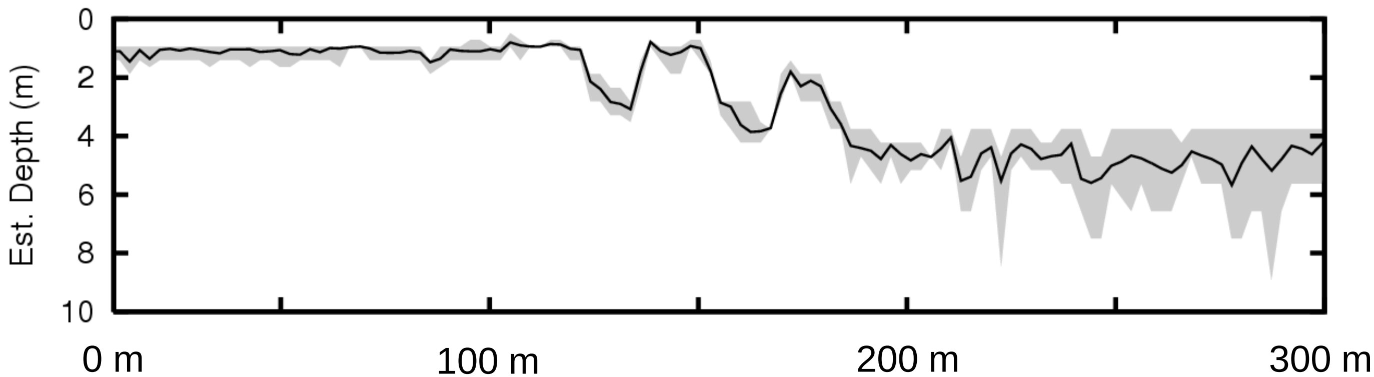

= 90% confidence interval

Sentinel-2 bathymetry of Lizard Island (GBR) by model inversion

- Uses bands 1, 2, 3, 4 and 5
- ALUT inversion of Lee et al. equations
- In-situ echo-sound data for comparison

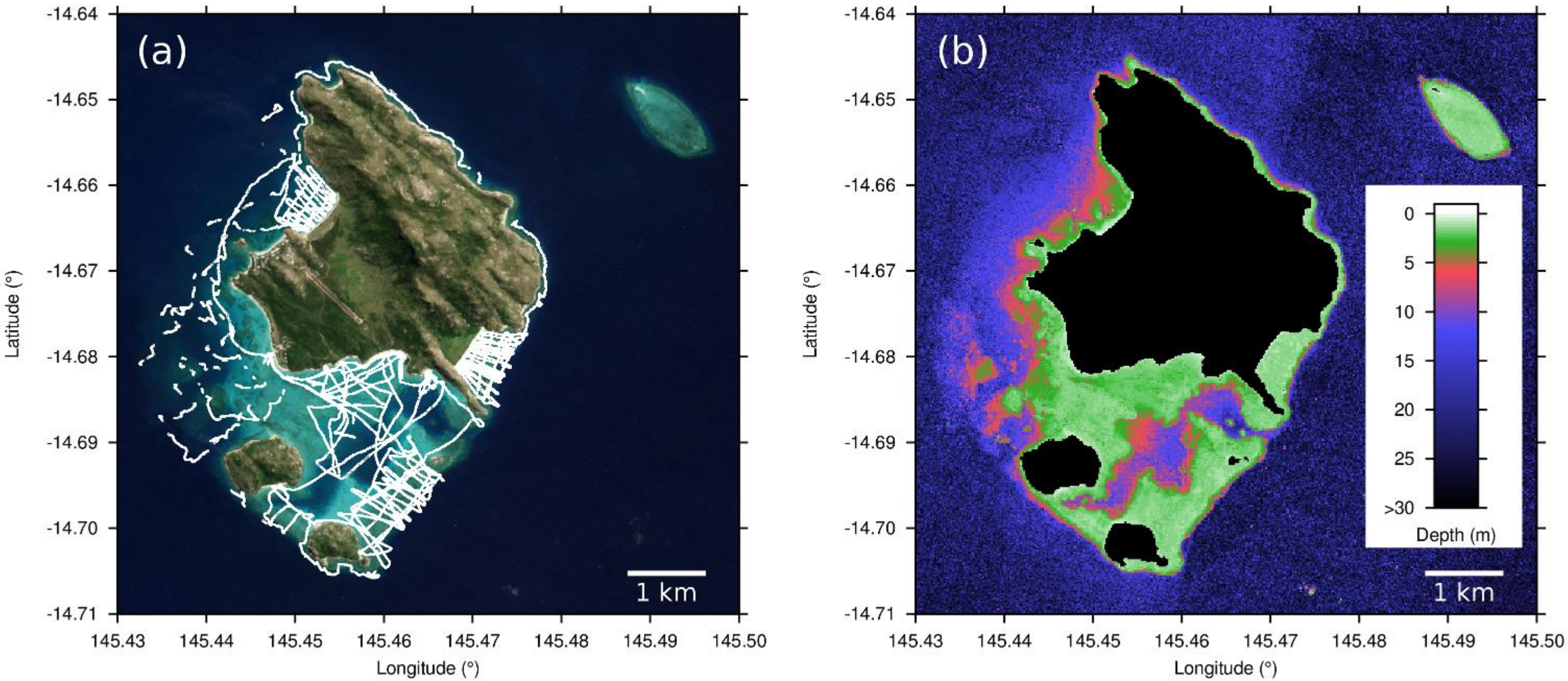

Single inversion vs. mean of noise perturbed inversions

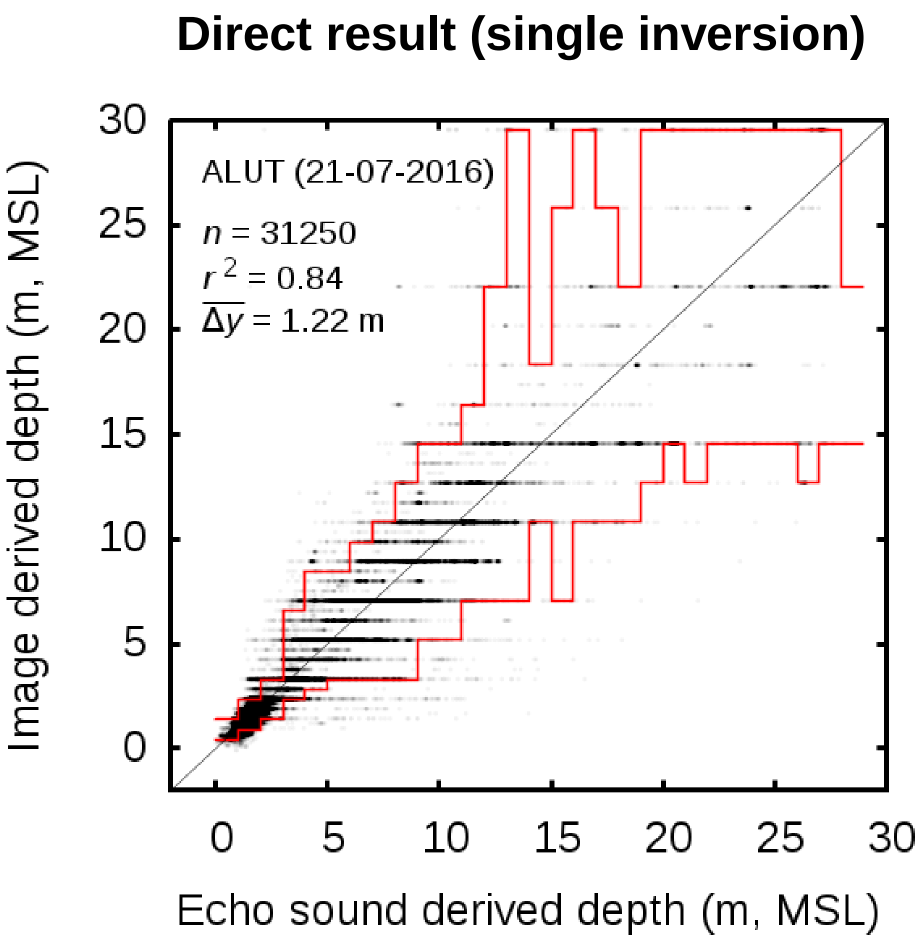

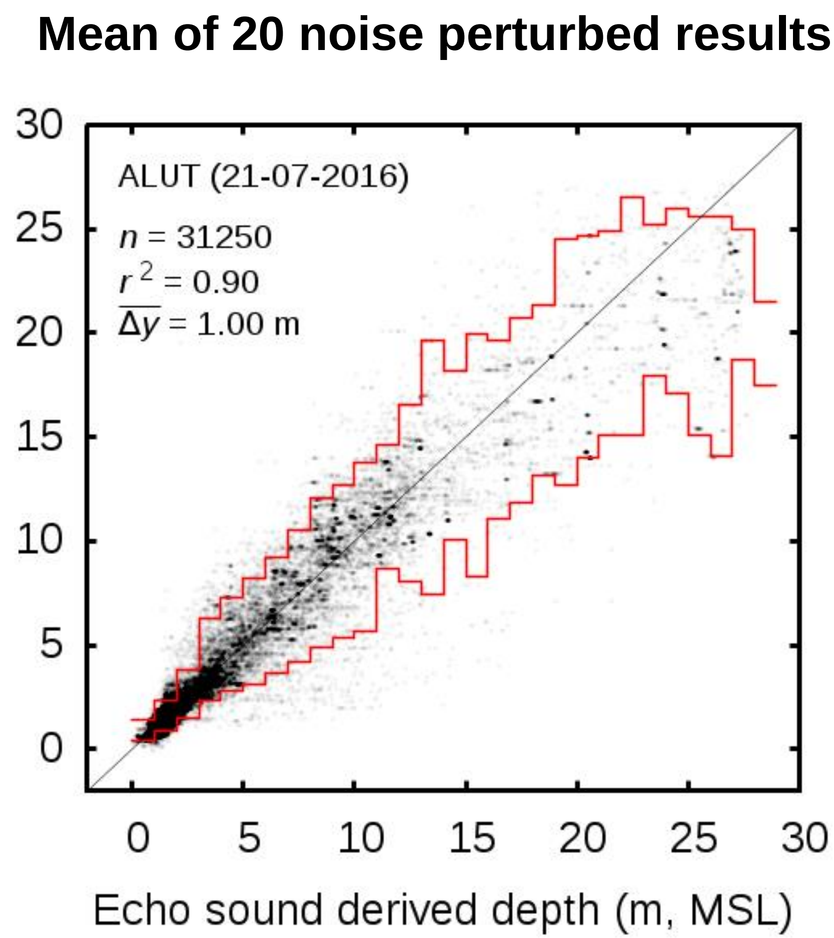

- Marginally better statistics, r-squared, mean absolute residual, etc.
- Cosmetically better (spatially smoother)

Bolinao, Philippines (QuickBird image)

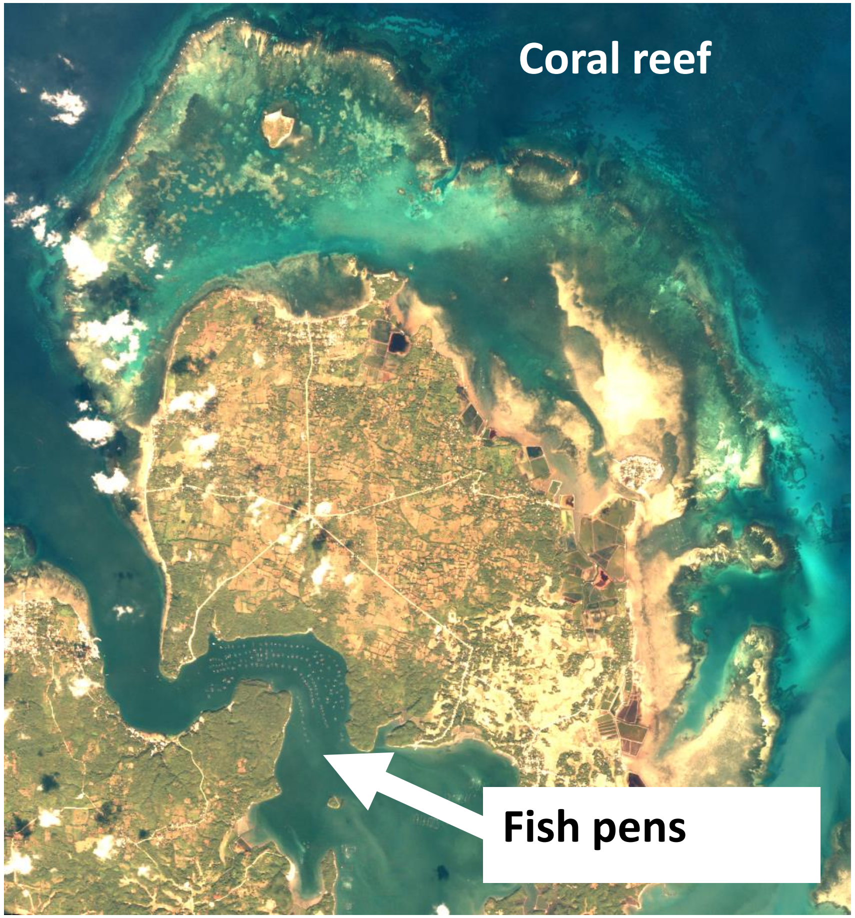

Coral Reef Targeted Research & Capacity Building for Management

MSI

Light absorption due to CDOM

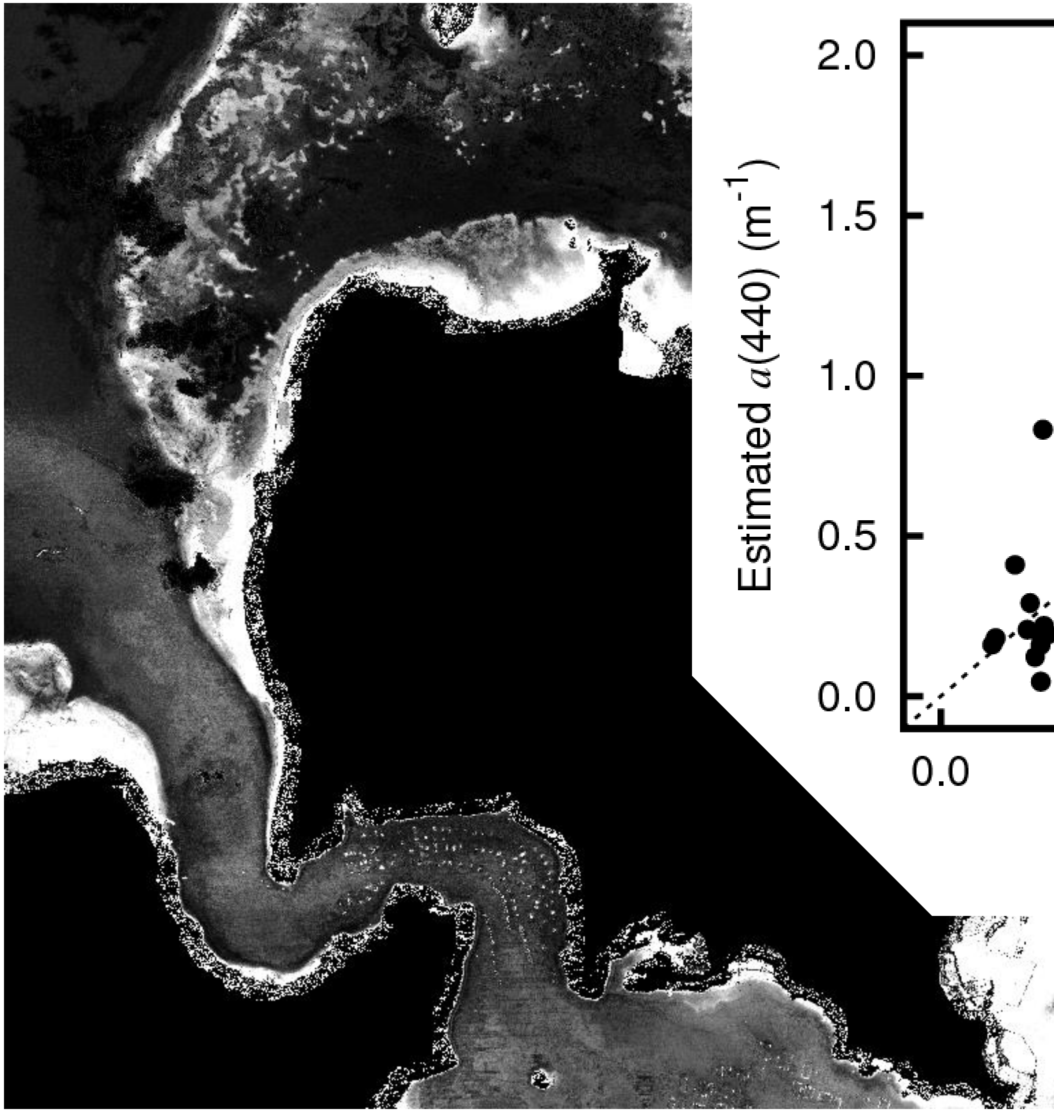

Total absorption

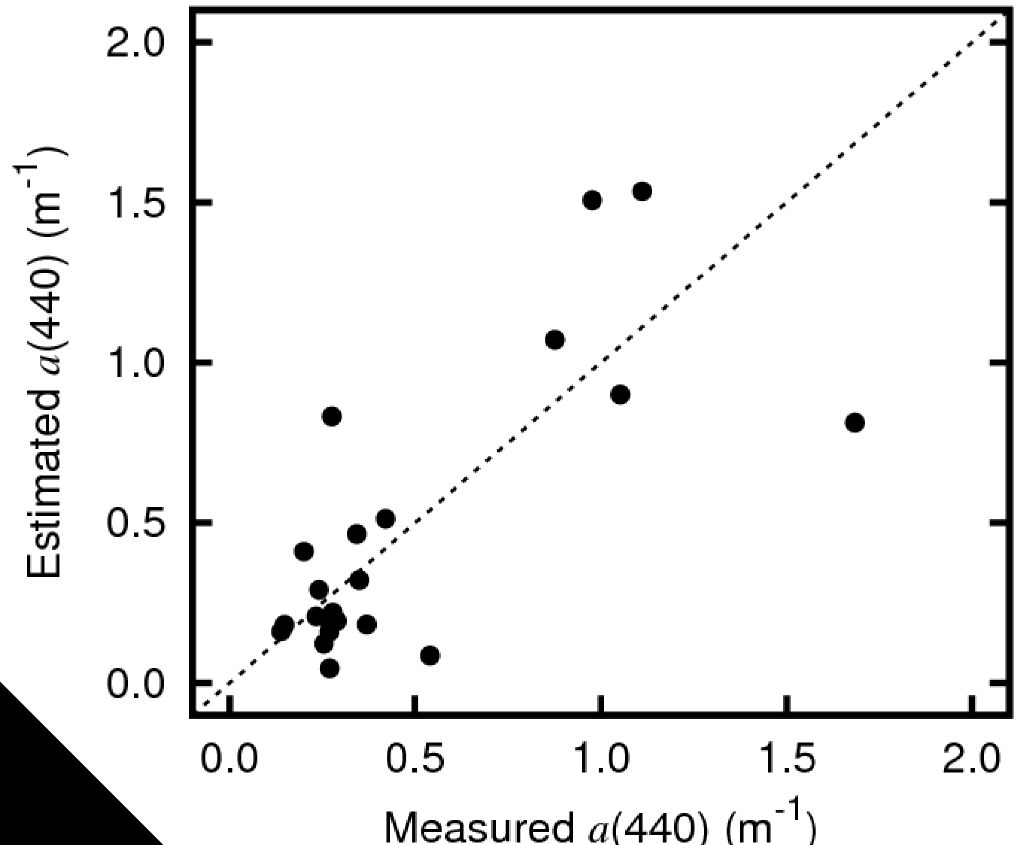

Light absorption due to CDOM

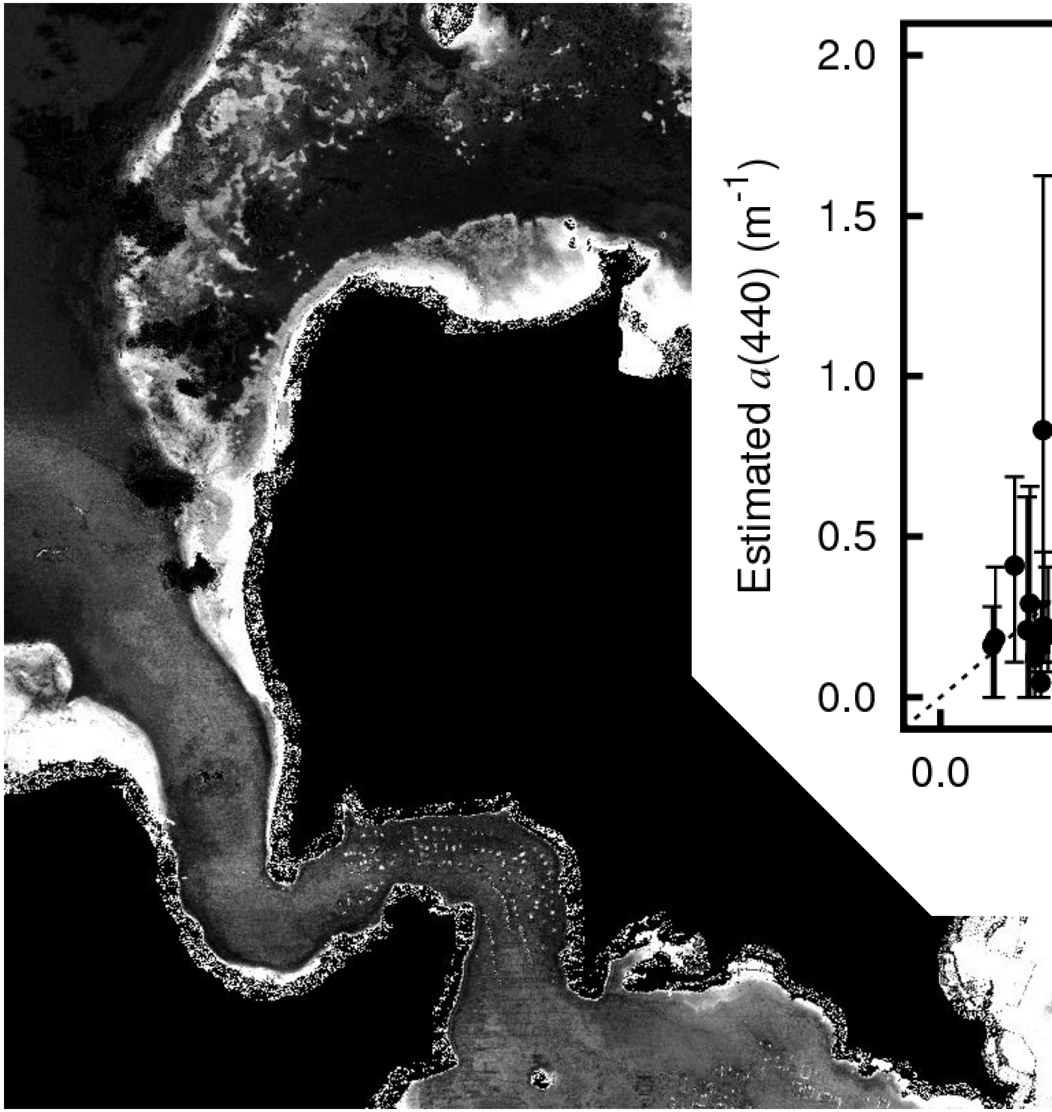

Total absorption

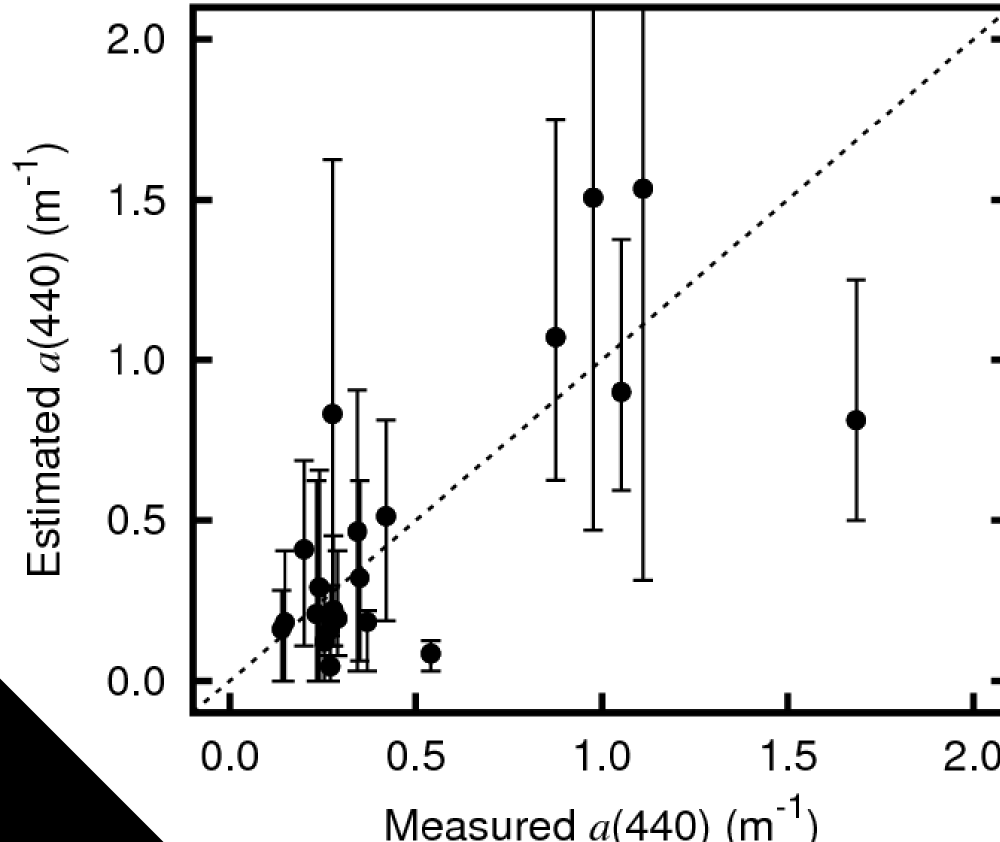

Bottom reflectance

- Either directly from the inversion or use the bathymetry estimate and water optical properties to make water column correction

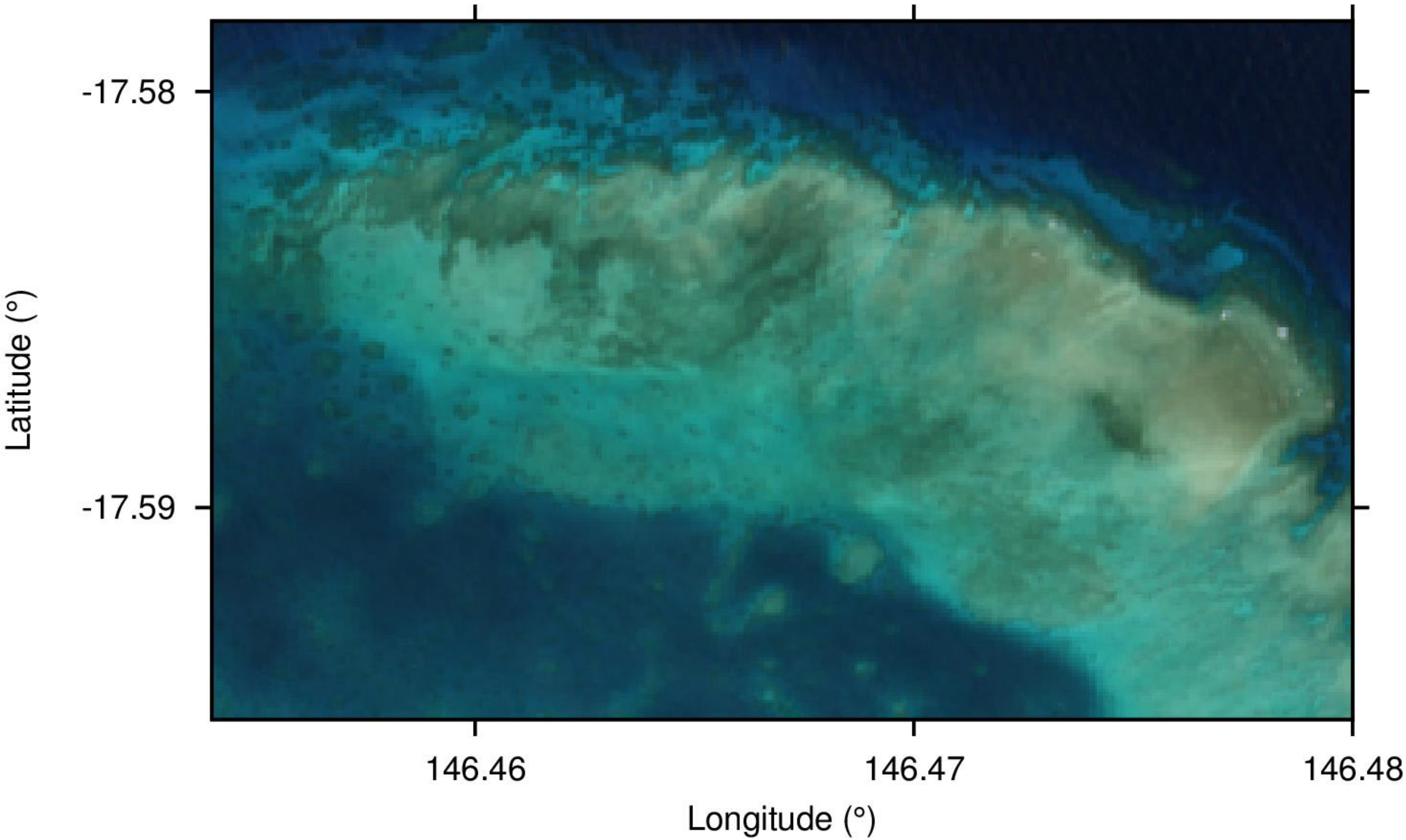

Bottom reflectance

- Either directly from the inversion or use the bathymetry estimate and water optical properties to make water column correction

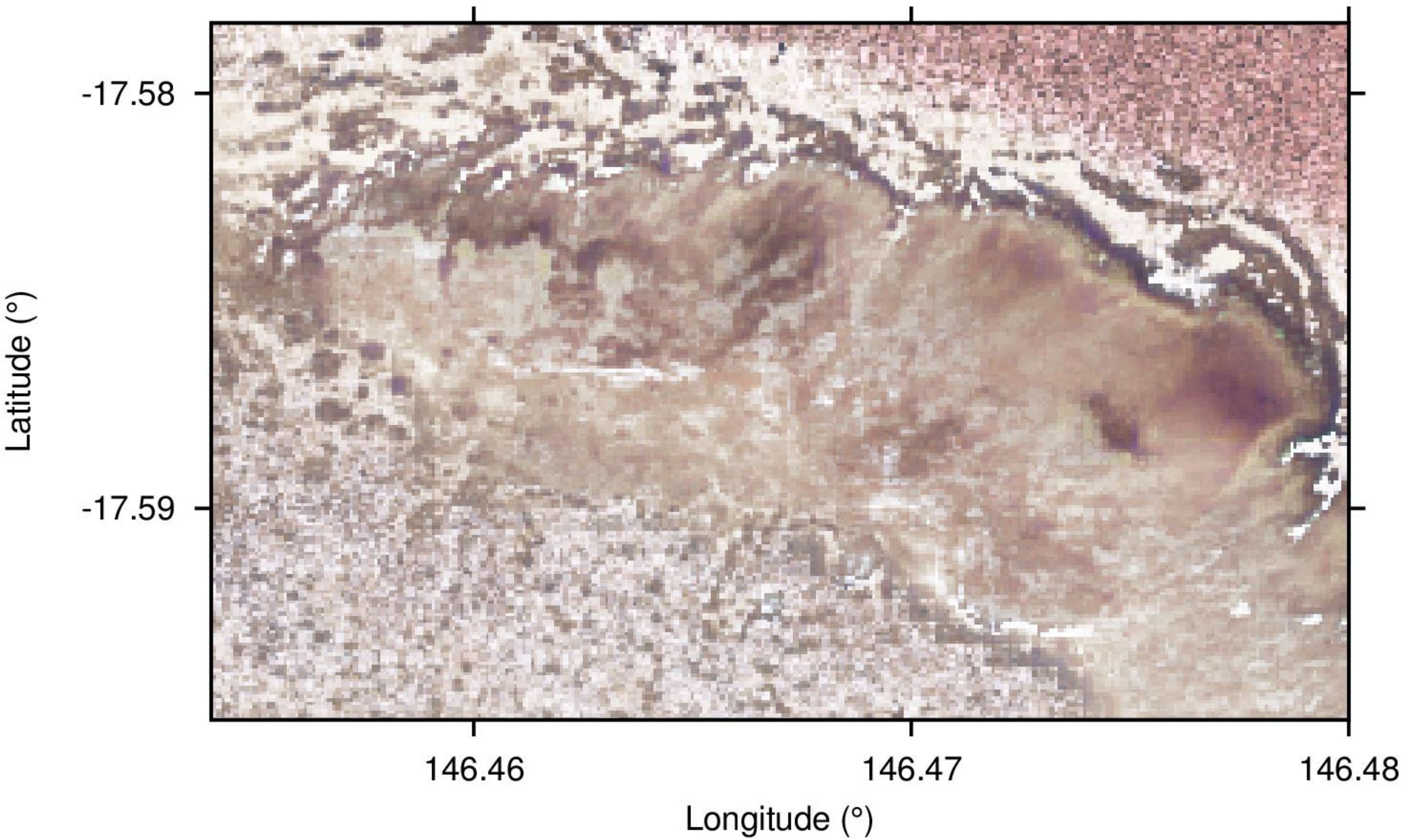

Canopy modelling, seagrass *Thalassia testudinium*

Low LAI

High LAI

- 3-dimensional geometric optics model
- Hedley & Enriquez, L&O 2010
- Hedley, Russell, Randolph & Dierssen, RSE 2016

➢ Reflectance above the canopy as a function of leaf area index (LAI)

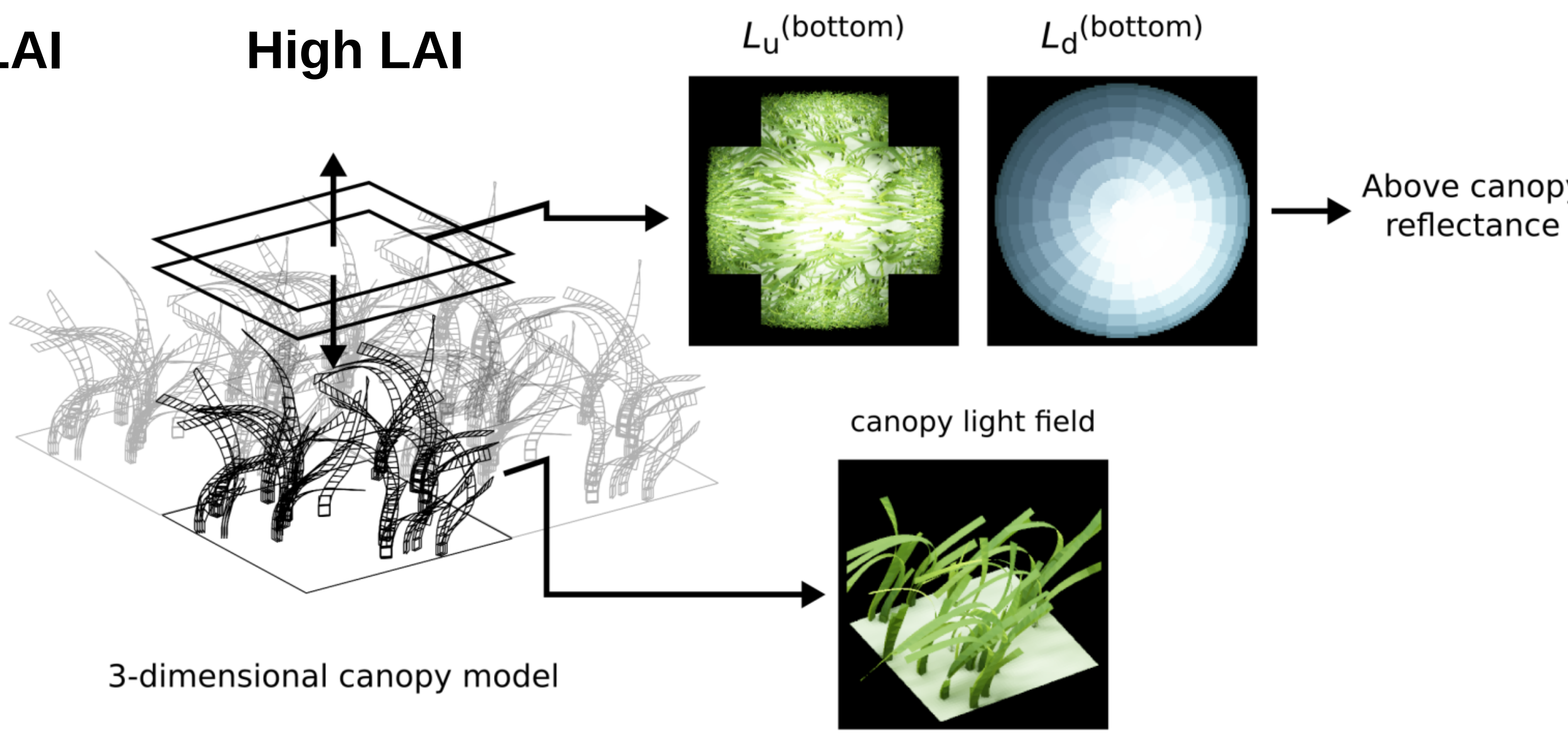

Leaf and sand optical properties

Reflectance and transmittance

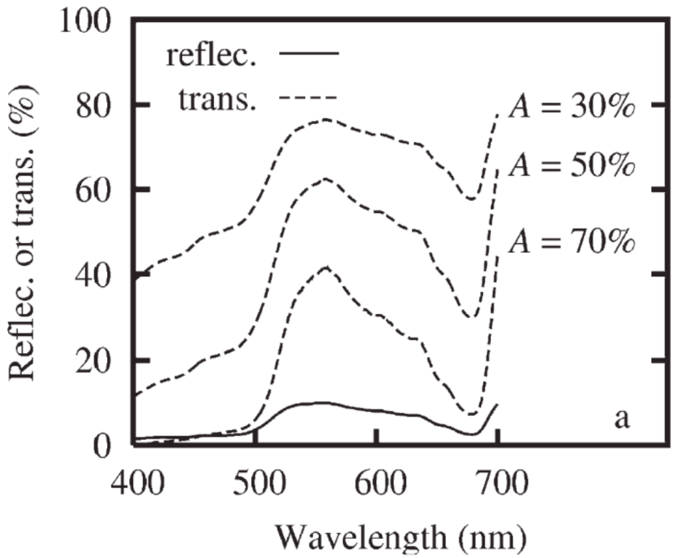

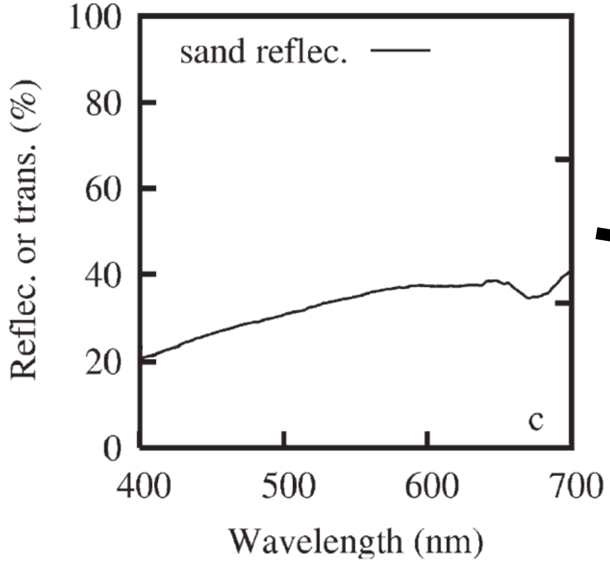

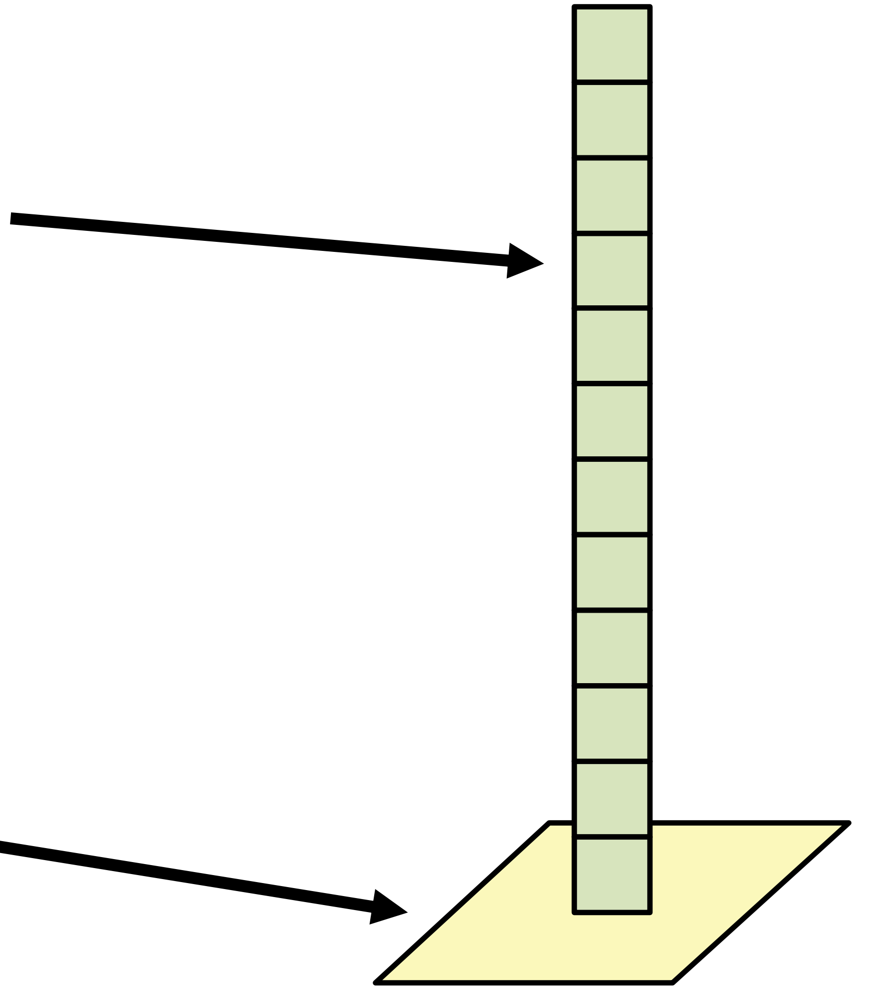

Canopy structure

- flexible strips in a simple wave motion model

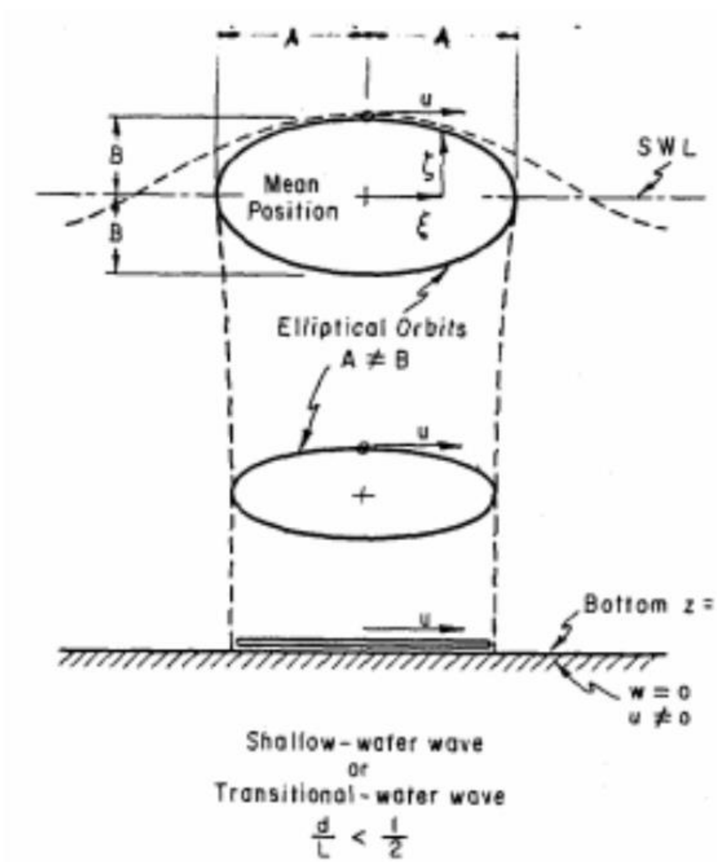

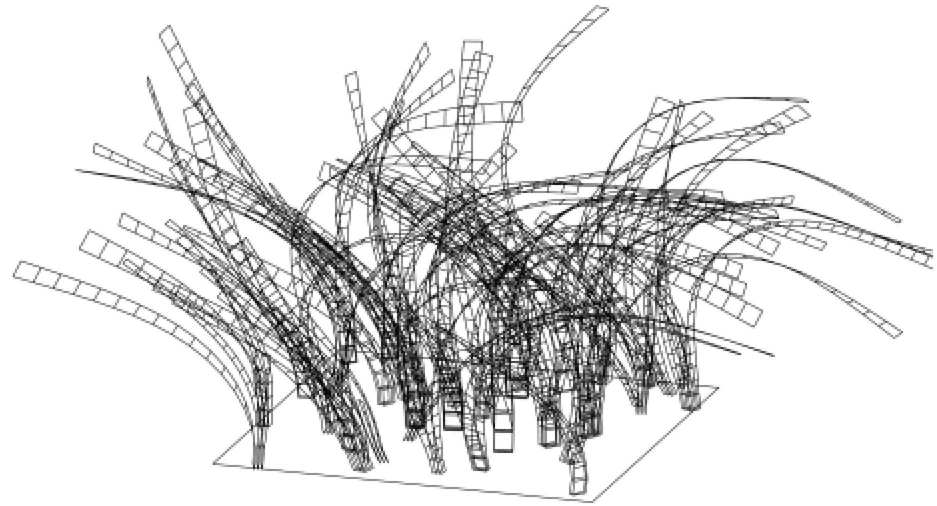

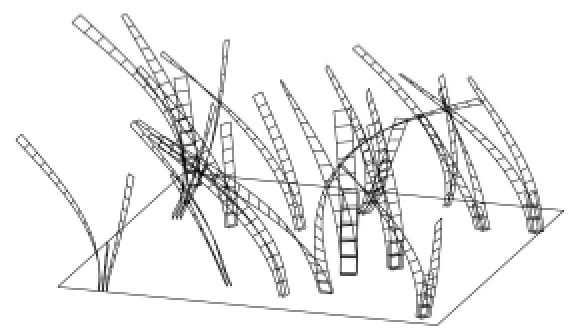

Canopy structure

- flexible strips in a simple wave motion model

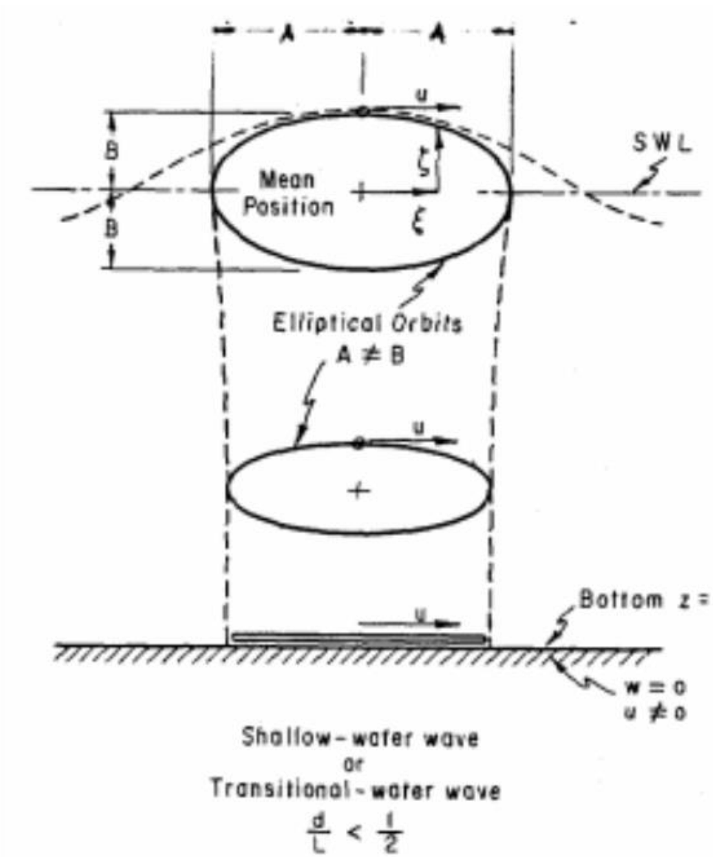

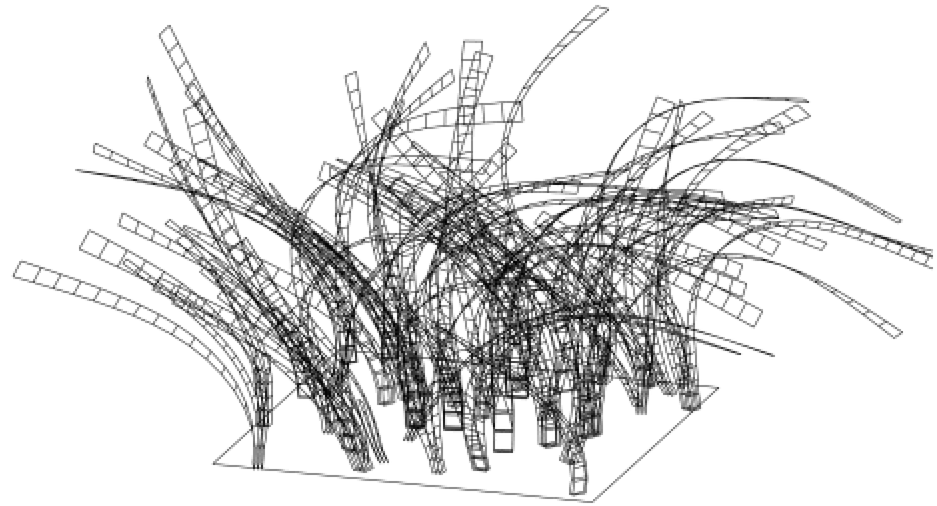

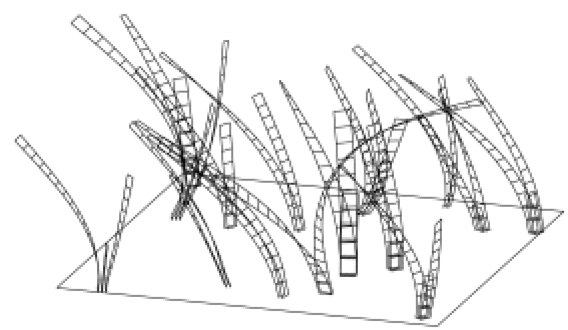

Model outputs (RGB from 17 bands)

LAI 4.5, depth 0.5 m

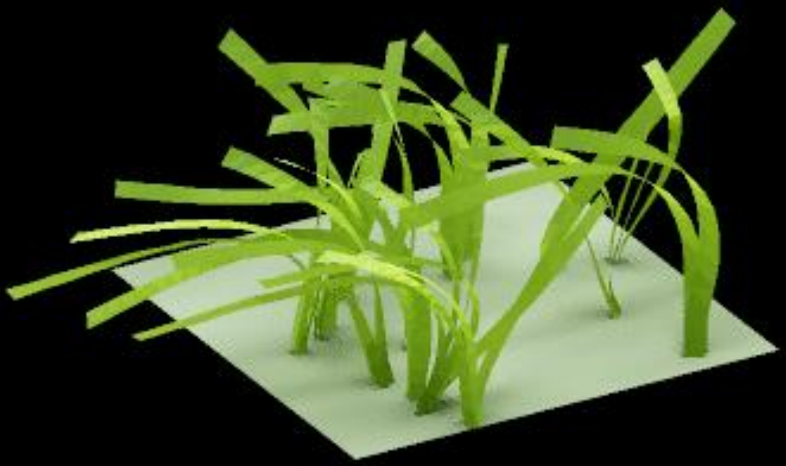

LAI 1.0, depth 1.5 m

Model outputs (RGB from 17 bands)

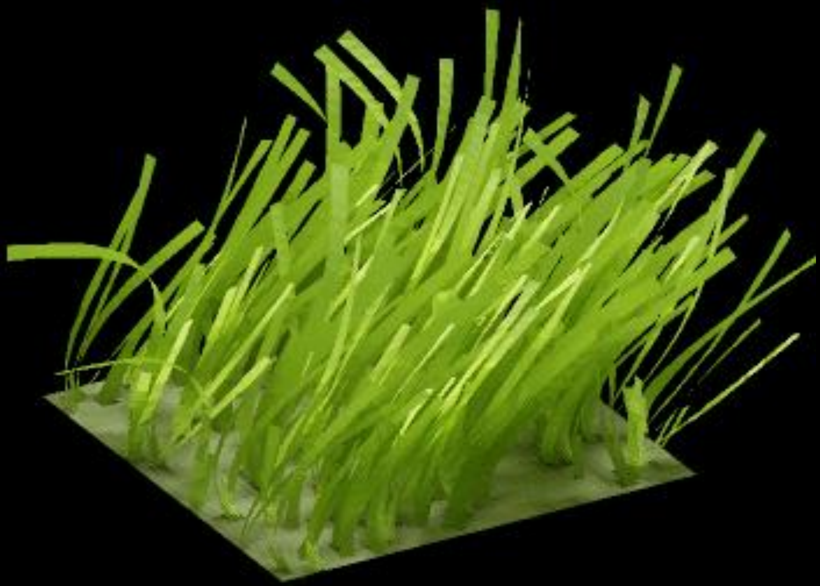

LAI 4.5, depth 0.5 m

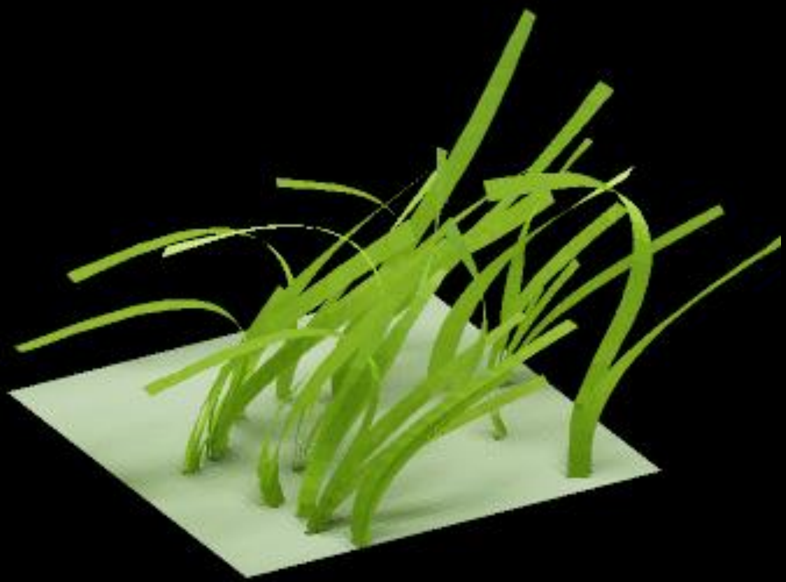

LAI 1.0, depth 1.5 m

Model many canopies with a multi-factor design

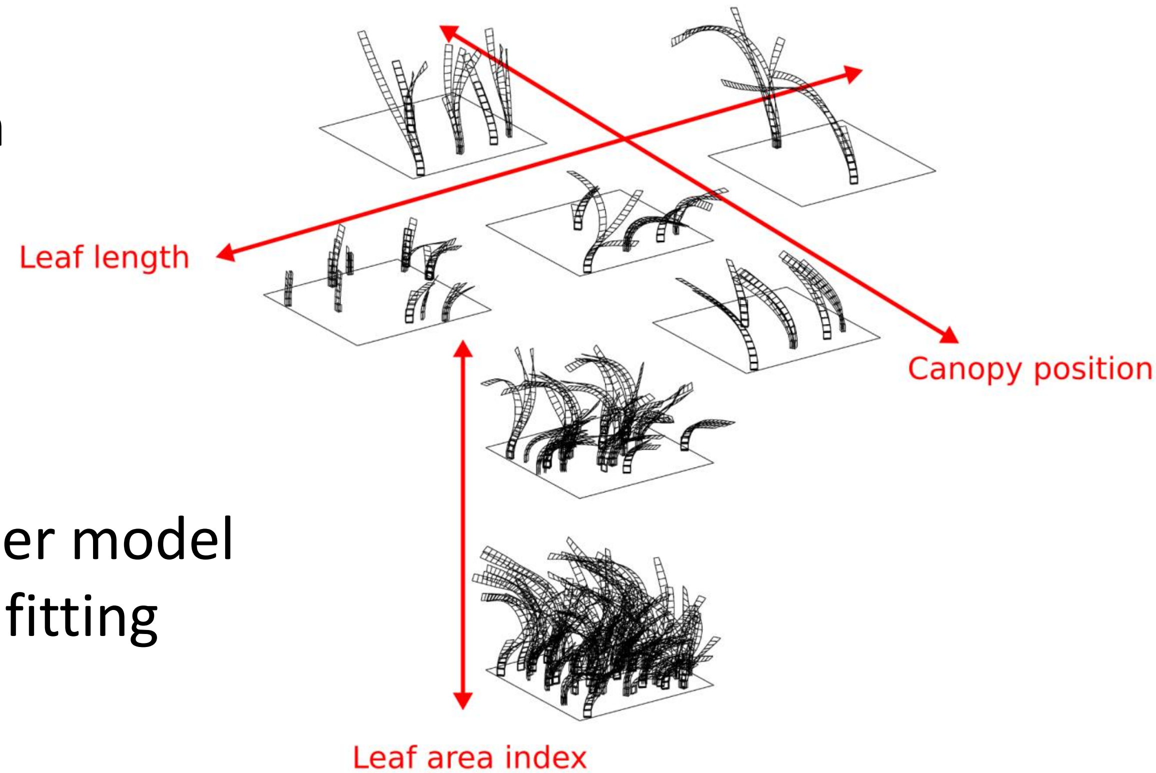

Reduce results to a simpler model by regression & function fitting

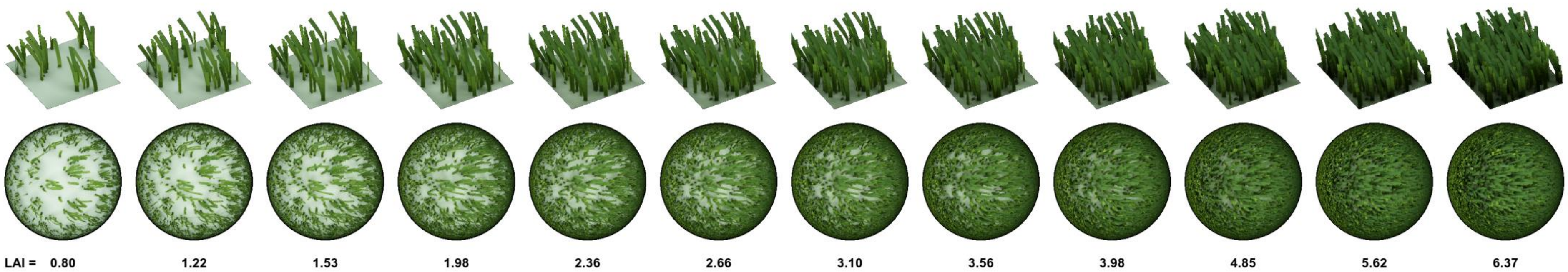

$$\rho(\lambda) \approx R_{\text{canopy}}(\text{LAI}, e, \lambda)$$

e is a parameter that ranges from 0 to 1 and encompasses the variation for a specific LAI

Other benthic metrics - seagrass density (leaf area index, LAI)

$$a(\lambda) = a_{\mathrm{w}}(\lambda) + \left[a_0(\lambda) + a_1(\lambda)\ln P\right] P + G \exp\left[-0.015\,(\lambda - 440)\right]$$

$$b_{\mathrm{b}}(\lambda) = b_{\mathrm{bw}}(\lambda) + X\,(400/\lambda)^{Y}$$

$$u(\lambda) = b_{\mathrm{b}}(\lambda) / \left[a(\lambda) + b_{\mathrm{b}}(\lambda)\right], \qquad \kappa(\lambda) = a(\lambda) + b_{\mathrm{b}}(\lambda)$$

$$r_{\mathrm{rs}}^{\mathrm{dp}}(\lambda) \approx \left[0.084 + 0.170 u(\lambda)\right] u(\lambda)$$

$$D_{\mathrm{u}}^{\mathrm{C}}(\lambda) \approx 1.03\sqrt{1 + 2.4u(\lambda)} \qquad D_{\mathrm{u}}^{\mathrm{B}}(\lambda) \approx 1.04\sqrt{1 + 5.4u(\lambda)}$$

remote sensing reflectance

$$r_{\mathrm{rs}}(\lambda) \approx r_{\mathrm{rs}}^{\mathrm{dp}}(\lambda)\left(1 - \exp\left\{-\left[\frac{1}{\cos\theta_{\mathrm{w}}} + \frac{D_{\mathrm{u}}^{\mathrm{C}}(\lambda)}{\cos\theta}\right]\kappa(\lambda) H\right\}\right) + \frac{1}{\pi}\rho(\lambda)\exp\left\{-\left[\frac{1}{\cos\theta_{\mathrm{w}}} + \frac{D_{\mathrm{u}}^{\mathrm{B}}(\lambda)}{\cos\theta}\right]\kappa(\lambda) H\right\}$$

bottom reflectance

$$\rho(\lambda) \approx R_{\mathrm{canopy}}(\mathrm{LAI}, e, \lambda)$$

Substitute bottom reflectance for a model based on LAI and variation term *e*

Gives a model that can be inverted directly for LAI

$$r_{\mathrm{rs}}(\lambda) \approx f(P, G, X, H, \mathrm{LAI}, e, \lambda)$$

Seagrass LAI mapping, Yucatán, Mexico

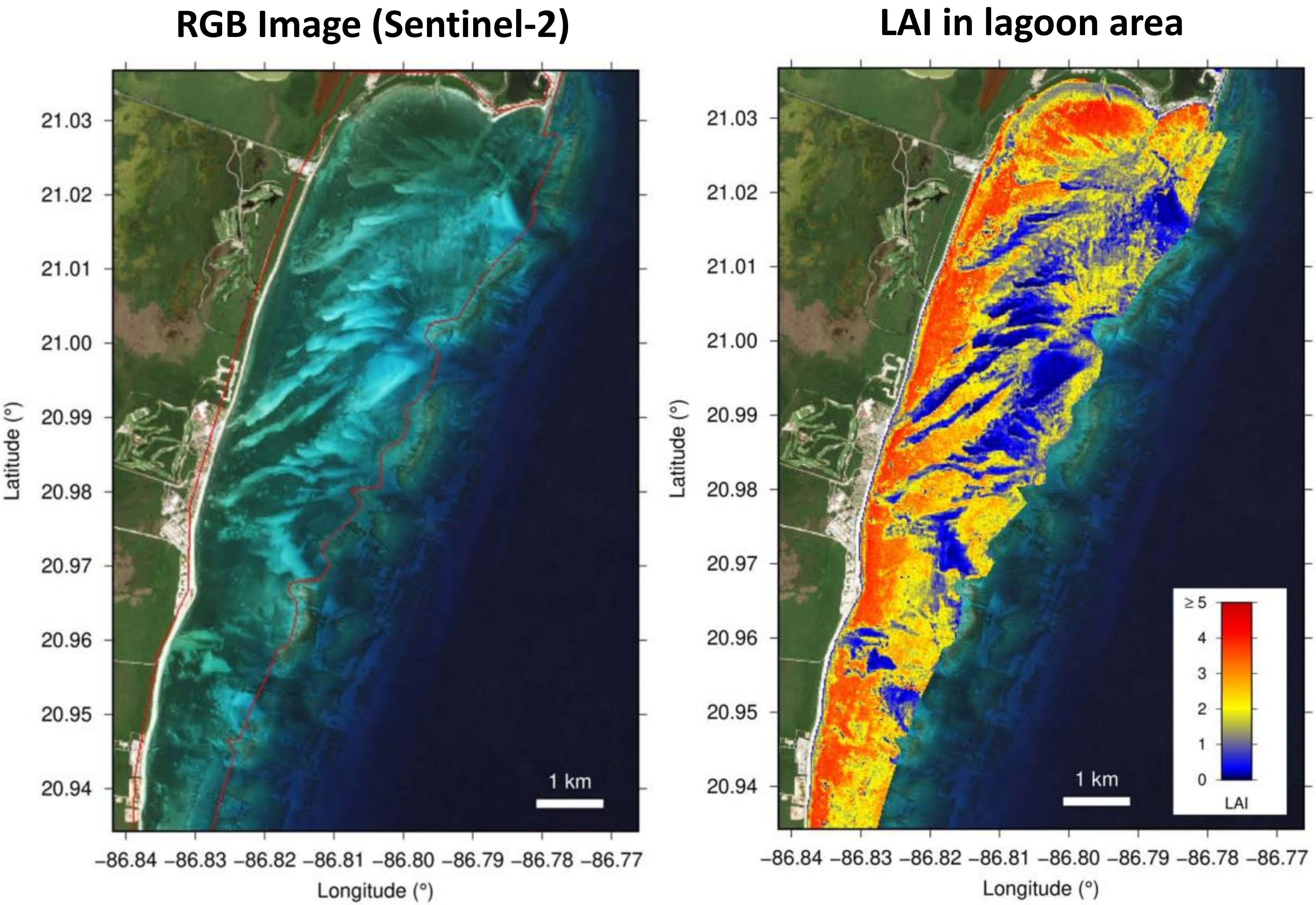

Hedley et al. 2021, *Frontiers in Marine Science*, 8, 733169 doi:10.3389/fmars.2021.733169

Difficulty in geo-locating ground truth data

Hard to survey at scales relevant to remote sensing

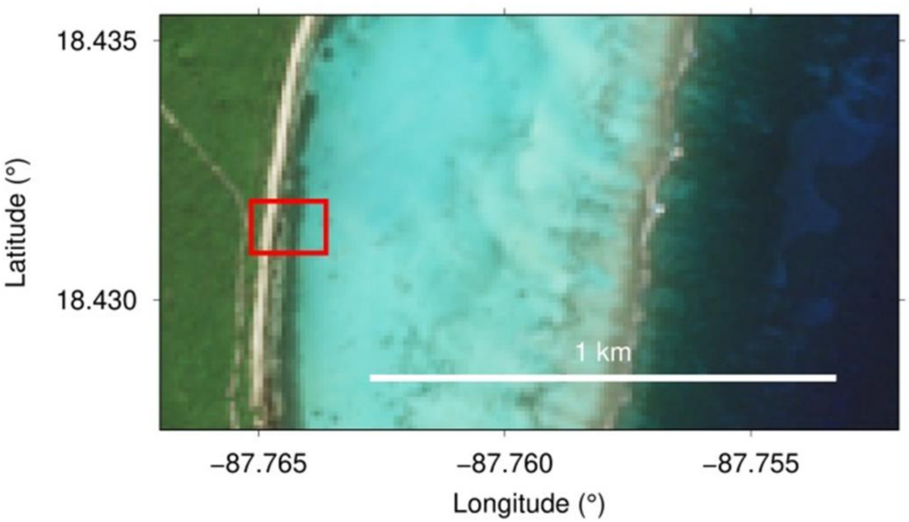

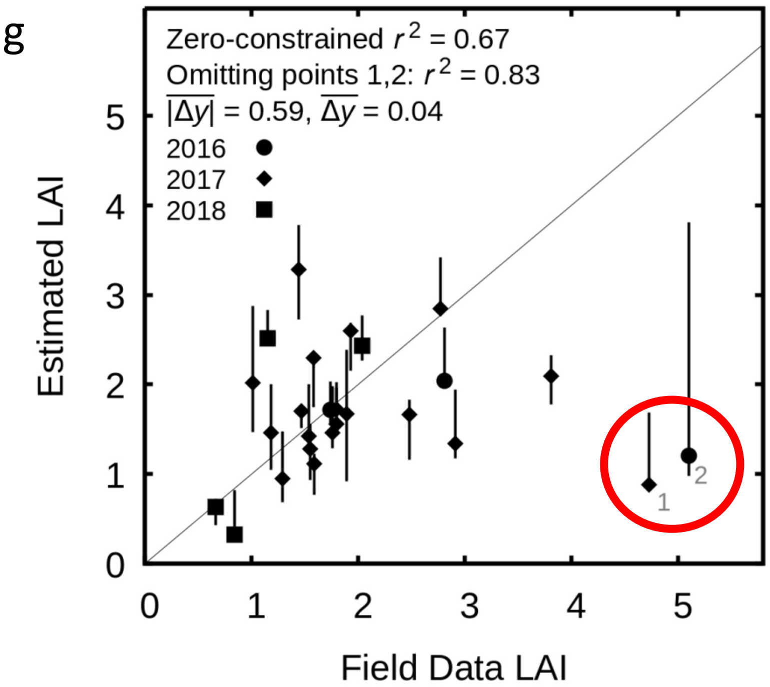

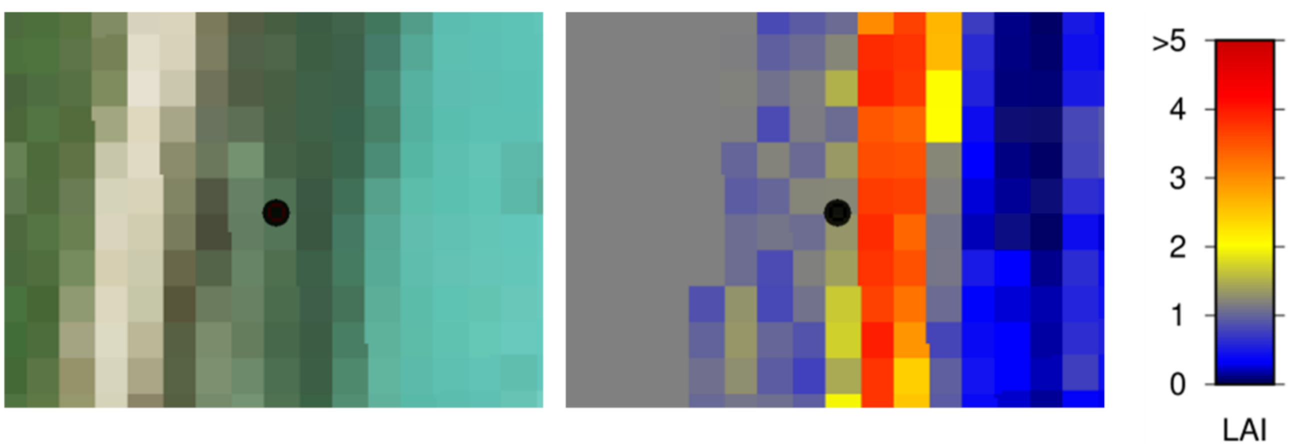

Hedley et al. 2021, *Frontiers in Marine Science*, 8, 733169 doi:10.3389/fmars.2021.733169

ICESat-2

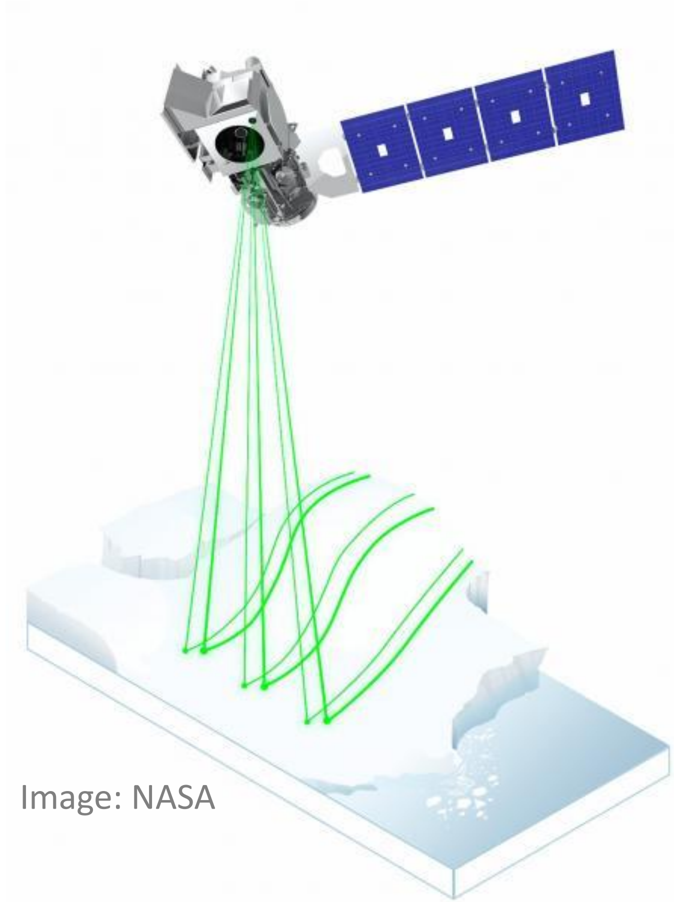

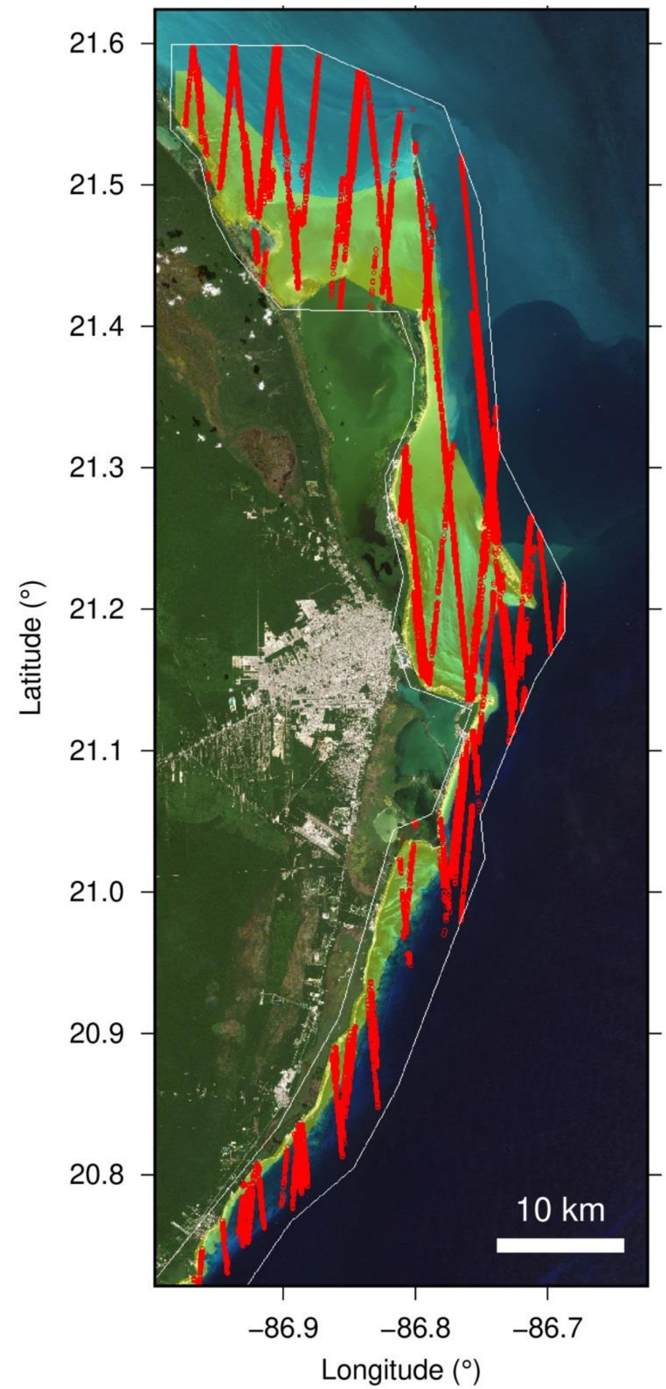

- Space-bourne LIDAR
- Launched 15 Sept. 2018
- Global acquisition
- Data freely available on on the web
- Possible to extract bathymetry

Typical ICESat-2 data

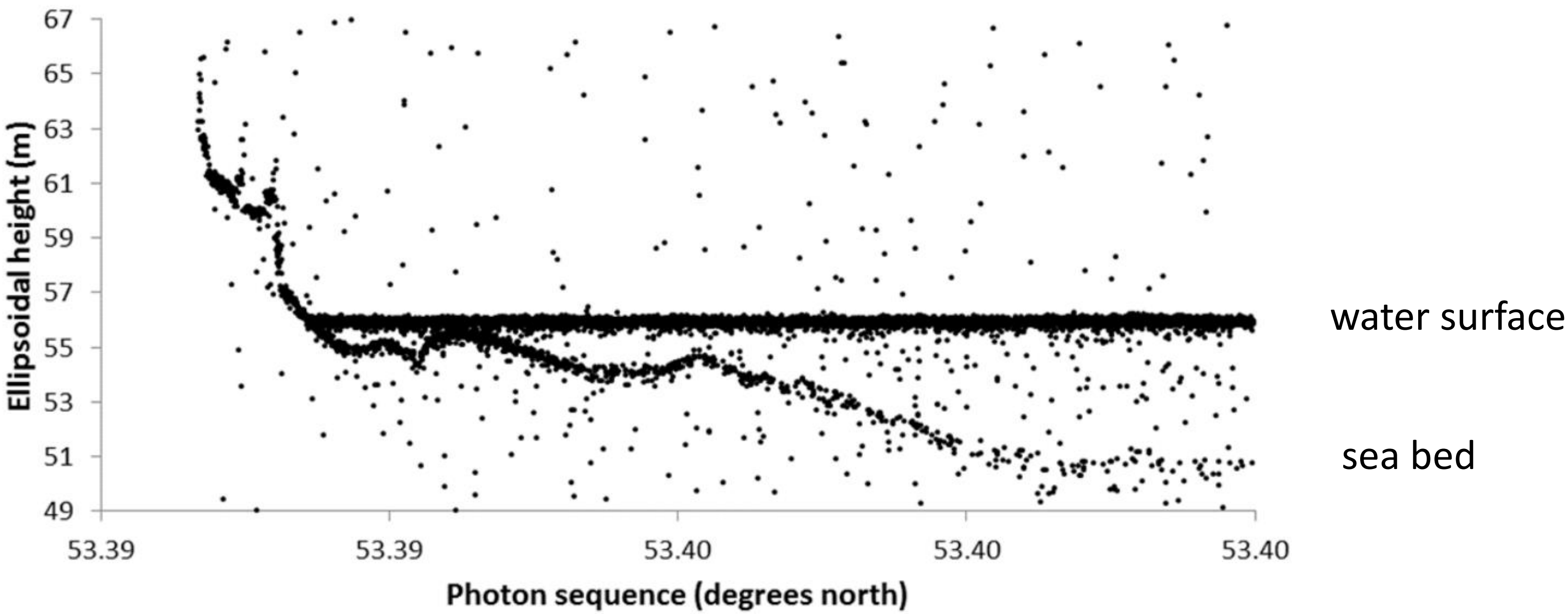

- Under favourable conditions depths to 20 m (or more) can be extracted
- Difficult to automate extraction
- Correct for refractive index, apparent depth is ~1.33 × depth

Coveney et al. 2021, *Remote Sensing*, 13, 4352; doi:10.3390/rs13214352

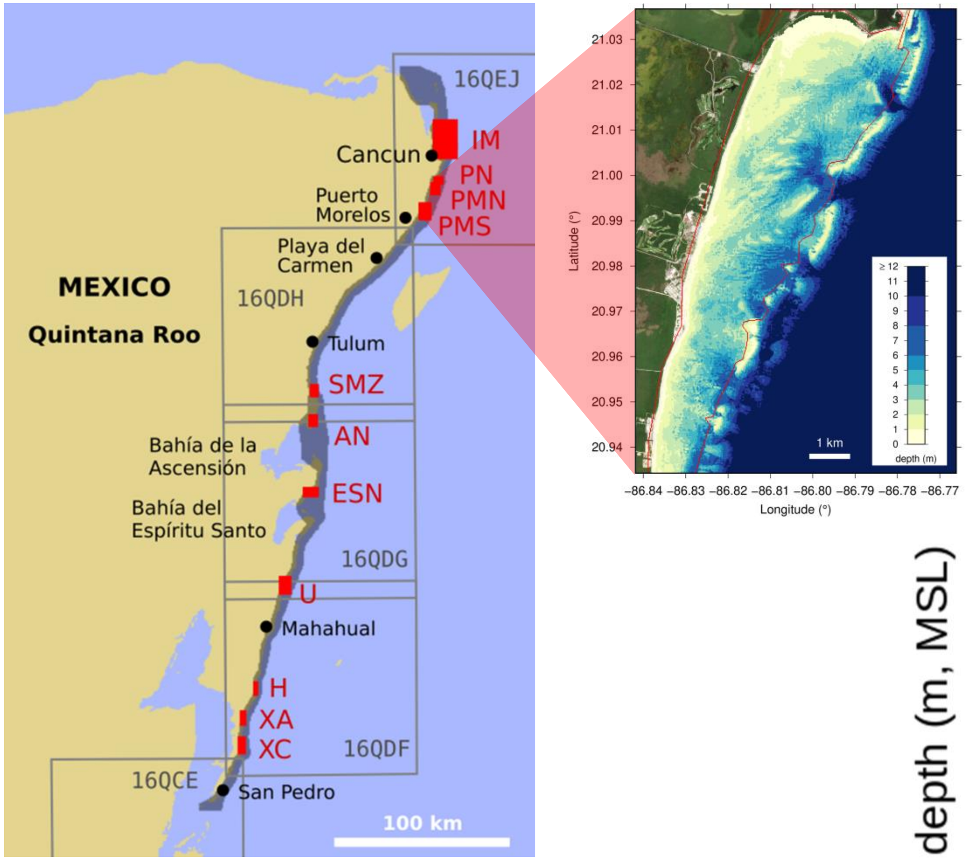

Comparison of model inversion bathymetry vs. ICESat-2 data for the entire Yucatan coast (~400 km)

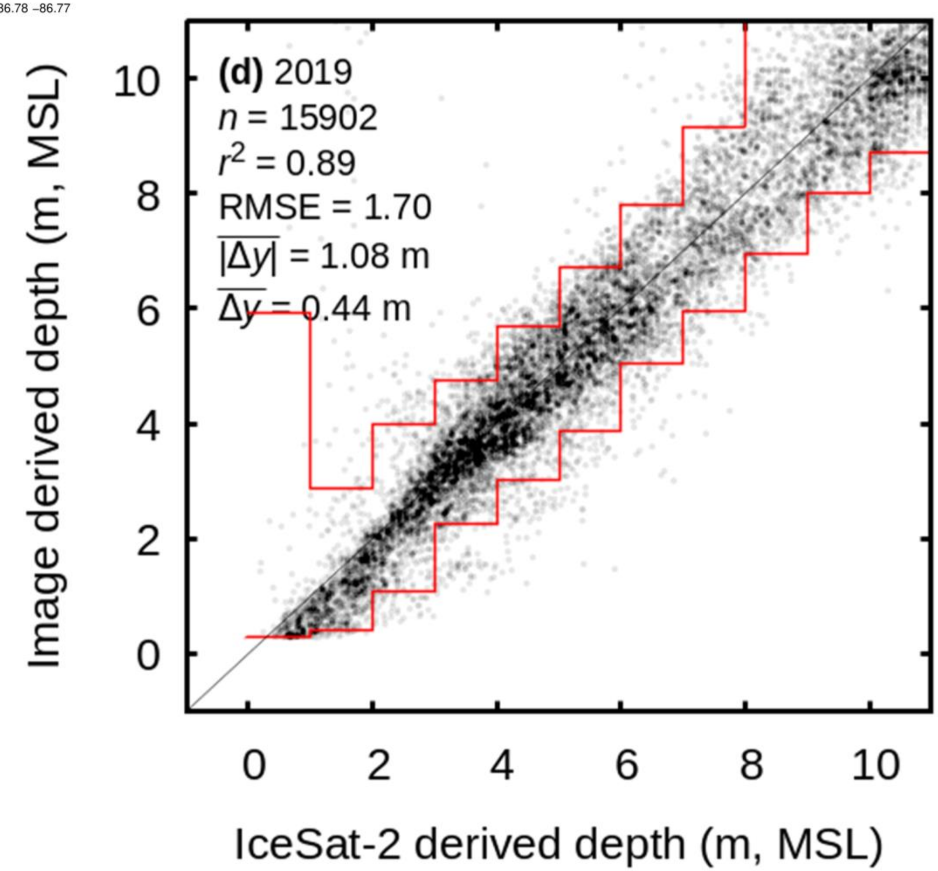

- Scale is more appropriate to remote sensing than echo sound data.
- Use data for calibration or validation?

Hedley et al. 2021, *Frontiers in Marine Science*, 8, 733169
doi:10.3389/fmars.2021.733169